

NACA RM L53K11



NACA

RESEARCH MEMORANDUM

EFFECTS OF A SERIES OF INBOARD PLAN-FORM MODIFICATIONS ON
THE LONGITUDINAL CHARACTERISTICS OF TWO UNSWEPT
WINGS OF ASPECT RATIO 3.5, TAPER RATIO 0.2,
AND DIFFERENT THICKNESS DISTRIBUTIONS
AT MACH NUMBERS OF 1.61 AND 2.01

By John R. Sevier, Jr.

Langley Aeronautical Laboratory
Langley Field, Va.

CLASSIFIED DOCUMENT

NATIONAL ADVISORY COMMITTEE
FOR AERONAUTICS

WASHINGTON

February 5, 1954

Classification changed (or changed to) Unclassified

by / author NASA Tech Pub Announcement #122
(OFFICER AUTHORIZED TO CHANGE)

BY 3 Dec 51

NK

CHANGED TO (or TO BE CHANGED TO)

21 Dec 51
DATE



NATIONAL ADVISORY COMMITTEE FOR AERONAUTICS

RESEARCH MEMORANDUM

EFFECTS OF A SERIES OF INBOARD PLAN-FORM MODIFICATIONS ON
THE LONGITUDINAL CHARACTERISTICS OF TWO UNSWEPT
WINGS OF ASPECT RATIO 3.5, TAPER RATIO 0.2,
AND DIFFERENT THICKNESS DISTRIBUTIONS
AT MACH NUMBERS OF 1.61 AND 2.01

By John R. Sevier, Jr.

SUMMARY

An investigation has been conducted at the Langley 4- by 4-foot supersonic pressure tunnel at Mach numbers of 1.61 and 2.01 to determine the effects of inboard plan-form modifications on two unswept wings. The two basic wings differed only in spanwise thickness distribution; the aspect ratio (3.5) and taper ratio (0.2) remained the same for both wings. Inboard plan-form modifications were made by means of insert sections which linearly extended the local chord, forward or rearward, from the 40 percent semispan station to the model center line.

Results of these tests indicated that addition of the extensions to either of the basic wings caused a reduction in minimum drag; theoretical calculations showed that these reductions can be predicted with reasonable accuracy. Although the extensions caused a decrease in lift-curve slope, (when based on wing areas including extensions) their over-all effect was to improve the maximum lift-drag ratio and to reduce the lift coefficient at which it occurred. Thus, by properly modifying the wing thickness and plan form, significant increases in wing volume (up to 80 percent for the configurations presented herein) could be attained with little or no penalties in drag and actual increases in maximum lift-drag ratio. Comparison of the present results with the results of a similar investigation for a 47° swept wing indicates that sweep angle has little effect on the relative improvements resulting from the addition of chord extensions.

~~CONFIDENTIAL~~*11-21-52*

INTRODUCTION

In references 1 to 4, an extensive investigation has been made to determine the effects of sweep and thickness on the aerodynamic characteristics of several wing-body combinations. A part of this general program was aimed at determining the practicability of increasing the wing volume by thickening the inboard part of the wing. For example, in reference 1, the inboard thickness ratios were increased on a 47° swept wing so that the wing volume was increased by 25 percent; results indicated that up to a Mach number of 0.88, no penalty in maximum lift-drag ratio was incurred for the thickened wing. At supersonic speeds, however, the effect of greater wave drag, associated with the increased thickness, was clearly evident in the reduced lift-drag ratios (refs. 3 and 4). Because of the practical advantages of the thicker wing, a further investigation was considered warranted to ascertain whether there were some practical means of maintaining its advantages at supersonic speeds.

A recent investigation of two 47° swept wings made at the Langley 4- by 4-foot supersonic pressure tunnel showed that, by properly modifying the wing thickness and plan form, significant increases in volume accompanied by actual increases in maximum lift-drag ratios, can be attained (ref. 5). One wing was of constant 6 percent thickness ratio throughout; whereas the other wing had the same sections outboard of the 40-percent-semispan station but inboard of this station, the thickness increased linearly to 12 percent at the model center line.

A less extensive investigation of a similar nature was made of a 45° swept wing by an Air Force contractor. The results of this investigation show the same general trends and are presented in reference 6.

In order to establish sweep effects, further tests (similar to those of ref. 5) were made of a wing which was unswept about the midchord line. Aspect ratio (3.5), taper ratio (0.2), and thickness distribution for the two basic wings remained the same as in reference 5. Results of this unswept-wing investigation are presented in the present report. Inboard plan-form modifications were effected by means of removable inserts which linearly extended the local chord, forward or rearward, from the 40-percent-semispan station to the model center line.

SYMBOLS

M	free-stream Mach number
q	free-stream dynamic pressure

S	area of wing extended through the fuselage to the center line
b	wing span
A	aspect ratio, b^2/S
c	airfoil chord at any spanwise station
y	spanwise distance measured from the plane of symmetry of the wing
\bar{c}	mean aerodynamic chord, $\frac{2}{S} \int_0^{b/2} c^2 dy$
α	angle of attack
L	lift
D	drag
C_L	lift coefficient, L/qS
$C_{L_{opt}}$	lift coefficient at maximum lift-drag ratio
C_D	drag coefficient, D/qS
$C_{D_{min}}$	minimum drag coefficient
C_m	pitching-moment coefficient about a line perpendicular to plane of symmetry and passing through the 25-percent position of the mean aerodynamic chord.
c.p.	center of pressure
C_{L_α}	lift-curve slope, per degree or per radian
C_{m_α}	pitching-moment-curve slope, per deg

WING DESIGNATION

In order to identify conveniently the various configurations tested, a three-unit numbering system has been adopted, each unit being separated from the others by a dash. The first number (6 or 12) designates the center-line thickness in percent chord of the basic wing; the second number (0, 33, 67, or 100) designates the percentage by which the basic center-line chord is extended by the forward insert; and the third number (0 or 33) refers to the percentage by which the basic center-line chord is extended by the rearward insert. Thus, the designation 6-0-0 refers to the basic 6-percent-thick wing, whereas the designation 12-100-33 refers to the 12-percent-thick wing with the basic center-line chord extended 100 percent forward and 33 percent rearward. In cases where a given number is variable, the number is replaced by X. Thus, when curves are plotted as a function of leading-edge extension, for example, for the 6-percent-thick wing with 33 percent rearward extension, the designation is 6-X-33.

APPARATUS

Tunnel

All tests were conducted in the Langley 4- by 4-foot supersonic pressure tunnel which is a rectangular, closed-throat, single-return wind tunnel designed for a nominal Mach number range of 1.2 to 2.2. The test-section Mach number is varied by deflecting horizontal flexible walls against a series of fixed interchangeable templates which have been designed to produce uniform flow in the test section. For the present investigation, the test-section Mach numbers were 1.61 and 2.01; the test-section heights were 4.4 feet and 5.1 feet, respectively; and the tunnel width was 4.5 feet.

Model

The test model consisted of either of two unswept wings (0° sweep about the midchord line) mounted on an ogive cylinder fuselage, the ogive having a fineness ratio of 3.5. The model was sting supported as shown in figure 1. Angle of attack was measured optically during each test and was varied by rotating the model about the balance-moment center. Although the fuselage housed a six-component internal strain-gage balance, only normal force, chord force, and pitching moment were analyzed.

The wings were constructed as indicated in figure 2. Outboard of the 40 percent semispan station, both wings were constructed of steel and had symmetrical $\frac{1}{3}$ - $\frac{1}{3}$ - $\frac{1}{3}$ hexagonal airfoil sections with a constant thickness

ratio of 6 percent. Inboard of the 40-percent-semispan station, the flat side of the hexagonal section was extended into the fuselage; the airfoil section over this inboard part was completed by the addition of any combination of forward and rearward inserts, as shown in figure 3.

Forward extensions of 33, 67, and 100 percent of the basic center-line chord and a rearward extension of 33 percent of the basic chord were tested in various combinations on each wing. Because of physical limitations of the model, the extensions tested in the present investigation were somewhat different from those of reference 5, in which forward and rearward extensions of 33 and 67 percent of the basic center-line chord were tested. It should be noted, however, that the maximum total chord extension remained the same.

The addition of chord extensions, to a wing of given thickness, necessarily changed the airfoil section because the thickness ratio and wedge angle were modified. Furthermore, when extensions were added which were nonsymmetrical forward and rearward, the section no longer remained a $\frac{1}{3} - \frac{1}{3} - \frac{1}{3}$ airfoil; its new shape depended on the particular combination of extensions. In short, the new airfoil was merely the basic airfoil with its three chord divisions elongated (either forward or rearward of the basic chord center line or both) by an amount dictated by the new wing designation; the increased length being allotted proportionally to the flat section and to the wedge section. The new airfoil sections can be derived by using the following relationships:

$$C_1 = \frac{\frac{1}{3}\left(1 + \frac{2A}{100}\right)}{1 + \frac{A + \beta}{100}}$$

$$C_2 = \frac{\frac{1}{3}\left(1 + \frac{A + B}{100}\right)}{1 + \frac{A + B}{100}} = \frac{1}{3}$$

$$C_3 = \frac{\frac{1}{3}\left(1 + \frac{2B}{100}\right)}{1 + \frac{A + B}{100}}$$

~~CONFIDENTIAL~~

where C_1 , C_2 , and C_3 are the lengths of the forward wedge, flat mid-section, and rearward wedge expressed as fractions of the new chord, and A and B are the percent forward and rearward extensions, respectively. Note that the flat section always remained one-third the chord.

Two sets of wings and insert extensions were tested. One wing with basic inserts (X-0-0) had constant 6-percent-thick sections throughout. The second wing with basic inserts was identical in plan form and had the same sections outboard of the 40-percent-semispan station as the 6-percent-thick wing. Inboard of the 40-percent-semispan station, however, the thickness increased linearly from 6 percent at the 40 percent station to 12 percent at the model center line. Since the 6-X-X and 12-X-X wings could both be tested with eight different combinations of inserts (fig. 3), there was a total of sixteen configurations tested.

Figure 4(a) shows the basic 6-percent-thick wing (6-0-0) and figure 4(b) shows the 6-percent-thick wing with 100 percent forward and 33 percent rearward extensions.

TESTS

All wing configurations shown in figure 3 were tested at a Mach number of 2.01 through an angle-of-attack range of -2° to 8° , approximately. The corresponding Reynolds number, based on the mean aerodynamic chord of the X-0-0 wing, was, with the exception of several isolated test conditions, 2.21×10^6 . For the extreme forward extensions, it was necessary to lower the tunnel stagnation pressure in order not to exceed the balance limit on pitching moment; for these configurations, the Reynolds number was 1.62×10^6 . A check run of the 12-0-0 wing at both Reynolds numbers indicated that there was no measurable effect due to this slight variation in Reynolds number.

In order to establish Mach number variation, the extreme configurations, shown in the corner sketches of figure 3, were also tested at a Mach number of 1.61. The Reynolds number for most of these tests was 2.68×10^6 ; for the most forward extensions, where it was necessary to lower the stagnation pressure, the Reynolds number was 1.42×10^6 .

Corrections were applied to all data in such a manner that the base pressure was corrected to free-stream static pressure. A 3-inch-diameter sting block (fig. 1) was used in order to minimize the base-pressure correction. The results of reference 5 indicated that the sting block had no effect on the final corrected data.

~~CONFIDENTIAL~~

THEORETICAL CALCULATIONS

Drag at Zero Lift

The drag at zero lift of each wing-body combination was considered to be the sum of the individual drags of the body and the exposed wing. Interference effects were neglected on the basis of the following considerations: (1) the body was cylindrical in the zone of influence of the wing and hence can experience no pressure drag in this region, and (2) the wing was operating in a flow field which was essentially uniform. The body pressure drag was calculated by means of linear theory as presented in reference 7. From tests of the body with and without a boundary-layer trip and from measurements made on a similar body in reference 3, the flow over the body was found to be turbulent. The skin friction, therefore, was estimated by the extended Frankl and Voishel method discussed in reference 8.

The wave drags of the basic wings (X-0-0) were calculated by linear theory by the use of a procedure similar to that outlined in references 9 and 10. For the extended-chord configurations, the wave-drag coefficients were estimated by a strip-theory calculation; that is, two-dimensional thickness corrections were applied to the basic wing to allow for the thickness-ratio changes as the inserts were added. No corrections were made for the plan-form change. The wing skin friction was estimated by the method of reference 11; laminar flow over the wing was assumed.

Lifting Characteristics

Although the lift-curve slopes of the wing and wing-body configuration are discussed separately in this section, it is to be emphasized that in the final presentation (where theory and experiment are compared), only the estimates for the wing-body combinations are presented. Calculations were made for the wing-alone configurations as a necessary step in obtaining the wing-body characteristics, however, no results for the wing alone are presented.

Wing lift-curve slope.— For the basic wing (X-0-0) alone, the lift-curve slopes were calculated directly from the expressions given in reference 12. In estimating them for the extended-chord configurations, certain simplifications were made in order to avoid prohibitively lengthy calculations. First, consider the X-0-33 configuration: since the trailing edge is supersonic, the addition of the 33 percent extension to the basic wing cannot affect the flow over the basic part of the new wing. Thus, the lift on the X-0-33 wing is merely the lift on the X-0-0 wing plus the lift on the added triangular area, which can be

calculated by integrating the theoretical linear pressures over the triangular part. This reasoning applies at both Mach numbers 1.61 and 2.01 because the trailing edge is supersonic in both cases. On the basis of the reversibility theorem (ref. 13), it is obvious that the X-33-0 configuration has the same theoretical lift-curve slope as the X-0-33 configuration. In order to obtain the lifting characteristics of the X-67-0 wing, the reverse flow is considered. At a Mach number of 2.01, the reverse-flow trailing edge of the insert is essentially sonic, hence the same method can be used as for the X-0-33 configuration. At a Mach number of 1.61, however, this reasoning does not apply, because the reverse-flow trailing edge is subsonic. Similarly, the lift-curve slopes of the X-100-0 wing cannot be calculated by these simple methods nor can calculations be made for configurations having a combination of forward and rearward extensions. That is, for configurations other than those discussed, the calculations were either prohibitively lengthy or were oversimplifications, therefore, no calculations of this type were carried out. It is believed, however, that the limited number of theoretical points calculated by the methods described are sufficient to establish agreement between experiment and theory and also to show that the general trends can be predicted reasonably well.

Wing-body lift-curve slope.- In estimating the effect of wing-body interference on the lift-curve slope, the method of reference 14 was used. For the basic wing, this method was applied directly, but for the extended-chord configurations, it was necessary to simplify the problem somewhat in order to avoid excessively lengthy calculations. For these configurations, then, it was assumed that the inboard section of the wing plan form was of primary importance in determining the effective lift carryover. Hence, the lift carryover was computed (by the use of ref. 12) for a wing of zero taper ratio having the same sweep of the leading and trailing edges as given by the insert sections.

Drag due to lift.- Because of the relative sharpness of the wing leading edge and the fact that the leading edge was supersonic, except for the cases of extreme forward extensions, the drag due to lift was assumed to be given by the component of normal force in the drag direction.

RESULTS AND DISCUSSION

Effects of Extensions on Unswept Wing

Basic data.- The basic lift, drag, and lift-drag-ratio data are presented as a function of angle of attack in figures 5 and 6 for both the 6-X-X and 12-X-X wing configurations. In addition, the lift-drag ratio data are plotted as a function of lift coefficient in figures 7 and 8.

The basic data for all the configurations tested are tabulated in table I. A summary of the individual wing characteristics (such as minimum drag and lift-curve slope) is presented in tables II and III.

Pitching-moment and center-of-pressure data are presented for the 6-X-X and 12-X-X wing series in figures 9 and 10, respectively. Since each insert section was assumed to form a new wing, a new moment center referenced to the quarter-chord point of the mean aerodynamic chord of each wing was used to reduce the data. Such referencing leads to the anomalous result that the forward extensions increase stability. This effect is due to the fact that the moment axis changes more rapidly than does the physical center of pressure, as is evident from the center-of-pressure data presented in figures 9 and 10.

Minimum drag coefficients.- In figure 11, the minimum drag coefficients for all the configurations tested are plotted as a function of the sum of the forward and rearward extensions. This presentation is consistent with the initial theoretical assumption that the extensions would introduce primarily a thickness effect. In figure 11(a), the drag coefficients have been based on the individual wing area, whereas in figure 11(b), the area of the basic wing (X-0-0) has been used to obtain drag coefficient. It should be emphasized that the significant reductions in minimum drag coefficient apparent from figure 11(a) are somewhat misleading since referencing a given drag force to a larger area (as extensions are added) will necessarily result in a lower coefficient. The picture is further distorted by the fact that the body drag, which is a large part of the total drag and is theoretically constant, is included in figure 11; the body drag, of course, is subject to the same misleading changes due to re-referencing. Hence, because of the re-referencing for each wing, it is difficult to make valid comparisons between configurations using figure 11(a). For this reason, figure 11(b) has been included in which the variation in minimum drag coefficient is equivalent to the variation in actual minimum drag since a common area has been used throughout.

The results of figure 11 indicate that the original thickness-correction concept is substantiated by the experimental data. That is, by the use of this thickness correction, it is possible to estimate reasonably well the variation in minimum drag coefficient with chord extensions.

Although the reduction in drag with chord extension (fig. 11(b)) is primarily a thickness effect, it is of interest to note the differences between two wings of the same thickness ratio; that is, to compare the 6-0-0 wing with the 12-67-33 wing, observing, of course, that both wings are of constant 6 percent thickness. Since the slight difference in airfoil section of the two wings in the inboard region introduces a negligible effect (based on two-dimensional linear-theory calculations),

then this comparison will indicate the effect of changing the plan form. Using tables II and III, the following results are obtained for a Mach number of 2.01:

Wing designation	$C_{D_{min}}$	$C_{D_{min}} \text{ X-0-0}$
6-0-0	0.0218	0.0218
12-67-33	.0167	.0223

Thus the 12-67-33 wing-body combination has only 2 percent more actual drag than the conventional 6-0-0 wing. Comparison of these two wings on the basis of volume indicates that the 12-67-33 wing has 67 percent greater volume (a parameter which may be extremely important) than the 6-0-0 wing. At a Mach number of 1.61, a comparison between the 6-0-0 and the 12-100-0 configurations (since the 12-67-33 configuration was not tested at the lower Mach number) indicated comparable results.

On the basis of limited comparisons, it was concluded that approximately the same percentage changes in minimum drag resulted from adding extensions to the swept-wing configurations (ref. 8) as to the present unswept configurations. The absolute drag values of the swept configurations were somewhat lower than those of the unswept ones at a Mach number of 1.61, but were essentially the same at a Mach number of 2.01.

Drag due to lift.- In figures 12 and 13, the drag-due-to-lift parameter is plotted as a function of forward chord extension for both the 6-X-X and 12-X-X wing series. As can be seen in figures 12(a) and 13(a), the reciprocal of the theoretical lift-curve slope (in radians) falls below the drag-due-to-lift parameter. This result can be attributed to the following conditions: (1) the resultant-force vector can be inclined at some angle other than normal (as was originally assumed), and (2) there might be inaccuracies in predicting the lift-curve slope. Subsequent plots show that there is good agreement between theoretical and experimental lift-curve slopes, therefore, the second reason is not a contributing factor in the present case. On the other hand, examination of figures 12(b) and 13(b) indicates that, in fact, the lift vector is inclined rearward of the normal to the chord. Thus, in the present case, the difficulty in predicting drag-due-to-lift characteristics lies in the fact that the original assumption of a normal lift vector is not strictly correct.

Lift-curve slopes.- Summary plots of the lift-curve slopes for all the wing-body configurations tested are presented in figures 14 and 15. As in previous summary plots, the parameter is based both on the individual wing area and on the area of the X-0-0 wing. Examination of figures 14 and 15 shows that there is very good agreement between experiment and theory, especially at the higher Mach number. Although the theoretical estimates presented are for a limited range, it can be concluded that reasonably accurate trends in lift-curve slope can be calculated by the use of the methods presented in this report.

Maximum lift-drag ratios.- The lift-drag-ratio data are presented as a function of forward chord extension in figures 16 and 17 for both the 6-X-X and 12-X-X wing series. In all cases, the addition of chord extensions to a wing of given thickness improved the maximum lift-drag ratio and, at the same time, reduced the lift coefficient at which it occurred. As can be seen from figures 16 and 17, the theoretical estimates of the maximum lift-drag ratio are somewhat high. These discrepancies are the result of accumulative small differences between experiment and theory in calculating lift, minimum drag, and drag due to lift. It should be noted that the trends between experiment and theory compare favorably although the actual values do not.

Again, it is of interest to compare the two 6-percent-thick wings (in combination with the body) at a Mach number of 2.01:

Wing designation	$\left(\frac{L}{D}\right)_{\max}$	$C_{L_{\text{opt}}}$
6-0-0	4.92	0.220
12-67-33	5.21	.185

Thus, the extended-chord wing configuration (which has 67 percent more volume) has a 6 percent higher maximum lift-drag ratio occurring at a lower lift coefficient and has only 2 percent more minimum drag than the basic configuration. Similar gains can be anticipated at a Mach number of 1.61.

Calculations of wing skin friction (with the assumption of laminar flow) indicate that this increase in maximum lift-drag ratio is chiefly a plan-form effect rather than a Reynolds number effect on skin friction (associated with the extended chord of the 12-67-33 wing). Further calculations show that even if the flow had been turbulent over the wings, the resulting increase in the level of skin friction and the larger

Reynolds number effect associated with the extended chord would be insufficient to cause any material effect on the percentage increases in maximum lift-drag ratio.

It is of importance to note that these data were obtained from relatively crude models designed to facilitate the testing of various arrangements. The results, therefore, are to be applied in order to indicate trends rather than for the specific numbers presented because, by using better airfoil sections, higher values in maximum lift-drag ratio could be realized.

Pitching-moment-curve slopes.- The pitching-moment-curve slopes and representative center-of-pressure locations for all configurations tested are presented in figures 18 and 19. The difficulty of considering each configuration as a new wing and relocating the moment axis is reflected in the pitching-moment-curve slopes; however, the representative center-of-pressure locations show the anticipated forward shift with forward extensions and rearward shift with rearward extensions.

Comparison Between the Swept and Unswept Wings

Although no specific curves showing sweep effects are presented in the present report, it will be of general interest to compare the basic swept and unswept wings, and to discuss the effects of adding extensions.

Sweep effects on the extended-chord configurations.- Because of basic differences between the tests of reference 5 and the present tests, only a limited number of extensions were common to both the swept and unswept wings. Thus, the conclusions regarding the effect of sweep will necessarily be based on limited comparisons. To be specific, at a Mach number of 1.61, the X-0-0 and X-0-33 configurations were common to both the swept and unswept wings; whereas, at a Mach number of 2.01, the X-0-0 and X-67-0 configurations were common to both. On the basis of these comparisons, it is concluded that at a Mach number of 1.61 the relative improvements due to adding extensions were essentially the same for the swept and unswept wings. At a Mach number of 2.01, it was found that slightly higher relative gains could be realized with the unswept wing.

Sweep effects on the basic wings.- Generally speaking, the aerodynamic characteristics of the 47° swept wing are better than those of the unswept wing; at least, over the Mach number range considered herein. At a Mach number of 1.61, the swept wing has definite advantages in minimum drag, drag due to lift, maximum lift-drag ratio, and optimum lift coefficient; however, at a Mach number of 2.01, these advantages are not as pronounced. For example, at the lower Mach number, the swept wing has 10 percent to 12 percent greater maximum lift-drag ratio, whereas,

at a Mach number of 2.01 this value has been reduced to about 5 percent. Similarly, the minimum drag of the basic swept wing is approximately 10 percent lower than that of the basic unswept wing at a Mach number of 1.61; whereas, at the higher Mach number the minimum-drag values of the two wings are essentially the same. Such trends substantiate the original assumption that the unswept wing would have better aerodynamic characteristics at the higher Mach numbers than the swept wing.

The only parameter considered herein which does not follow this pattern is lift-curve slope. At a Mach number of 1.61, the lift-curve slope of the unswept wing is about 10 percent higher than that for the swept wing, whereas at a Mach number of 2.01, the two are approximately the same.

CONCLUDING REMARKS

An investigation has been conducted at the Langley 4- by 4-foot supersonic pressure tunnel at Mach numbers of 1.61 and 2.01 to determine the effects of inboard plan-form modifications to two unswept wings. The two basic wings differed only in spanwise thickness distribution; the aspect ratio (3.5) and taper ratio (0.2) remained the same for both wings. Inboard plan-form modifications were made by means of insert sections which linearly extended the local chord, forward or rearward, from the 40-percent-semispan station to the model center line.

Results of these tests indicated that addition of the extensions to either of the basic wings caused a reduction in minimum drag; theoretical calculations showed that these reductions could be predicted with reasonable accuracy. Although the extensions caused a decrease in lift-curve slope (when based on wing areas including extensions), their over-all effect was to improve the maximum lift-drag ratio and to reduce the lift coefficient at which it occurred. Thus, by properly modifying the wing thickness and plan form, significant increases in wing volume (up to 80 percent for the configurations tested herein) can be attained with little or no penalties in drag and actual increases in maximum lift-drag ratio.

Comparison of the present results with the results of a similar investigation for a 47° swept wing indicates that sweep angle has little effect on the relative improvements resulting from the addition of chord extensions.

Langley Aeronautical Laboratory,
National Advisory Committee for Aeronautics,
Langley Field, Va., October 28, 1953.

~~CONFIDENTIAL~~

REFERENCES

1. Harris, William G.: A Wind-Tunnel Investigation at High-Subsonic and Low-Supersonic Mach Numbers on a Series of Wings With Various Sweepback, Taper, Aspect Ratio, and Thickness. AF Tech. Rep. No. 6669, Pt. 1, Wright Air Dev. Center, U. S. Air Force, Oct. 1951.
2. Bielat, Ralph P., Harrison, Daniel E., and Coppolino, Domenic A.: An Investigation at Transonic Speeds of the Effects of Thickness Ratio and of Thickened Root Sections on the Aerodynamic Characteristics of Wings With 47° Sweepback, Aspect Ratio 3.5, and Taper Ratio 0.2 in the Slotted Test Section of the Langley 8-Foot High-Speed Tunnel. NACA RM L51I04a, 1951.
3. Robinson, Ross B., and Driver, Cornelius: Aerodynamic Characteristics at Supersonic Speeds of a Series of Wing-Body Combinations Having Cambered Wings With an Aspect Ratio of 3.5 and a Taper Ratio of 0.2 - Effects of Sweep Angle and Thickness Ratio on the Aerodynamic Characteristics in Pitch at $M = 1.60$. NACA RM L51K16a, 1952.
4. Robinson, Ross B.: Aerodynamic Characteristics at Supersonic Speeds of a Series of Wing-Body Combinations Having Cambered Wings With an Aspect Ratio of 3.5 and a Taper Ratio of 0.2. Effects of Sweep Angle and Thickness Ratio on the Aerodynamic Characteristics in Pitch at $M = 2.01$. NACA RM L52E09, 1952.
5. Cooper, Morton, and Sevier, John R., Jr.: Effects of a Series of Inboard Plan-Form Modifications on the Longitudinal Characteristics of Two 47° Sweptback Wings of Aspect Ratio 3.5, Taper Ratio 0.2, and Different Thickness Distributions at Mach Numbers of 1.61 and 2.01. NACA RM L53E07a, 1953.
6. Mardin, H. R.: Supersonic Wind Tunnel Tests of the 0.02 Scale Full Span Model of the NA-180 (YF-100A) Airplane Through a Mach Number Range of 0.70 to 2.87 To Determine the Effect of Modifications to the Basic Model Components on the Aerodynamic Characteristics. Rep. No. SAL-43, North American Aviation, Inc., Oct. 30, 1952.
7. Lighthill, M. J.: Supersonic Flow Past Bodies of Revolution. R. & M. No. 2003, British A.R.C., 1945.
8. Rubesin, Morris W., Maydew, Randall C., and Varga, Steven A.: An Analytical and Experimental Investigation of the Skin Friction of the Turbulent Boundary Layer on a Flat Plate at Supersonic Speeds. NACA TN 2305, 1951.

9. Nielsen, Jack N.: Effect of Aspect Ratio and Taper on the Pressure Drag at Supersonic Speeds of Unswept Wings at Zero Lift. NACA TN 1487, 1947.
10. Beane, Beverly: The Characteristics of Supersonic Wings Having Biconvex Sections. Jour. Aero. Sci., vol. 18, no. 1, Jan. 1951, pp. 7-20.
11. Chapman, Dean R., and Rubesin, Morris W.: Temperature and Velocity Profiles in the Compressible Laminar Boundary Layer With Arbitrary Distribution of Surface Temperature. Jour. Aero. Sci., vol. 16, no. 9, Sept. 1949, pp. 547-565.
12. Lapin, Ellis: Charts for the Computation of Lift and Drag of Finite Wings at Supersonic Speeds. Rep. No. SM-13480, Douglas Aircraft Co., Inc., Oct. 14, 1949.
13. Brown, Clinton E.: The Reversibility Theorem for Thin Airfoils in Subsonic and Supersonic Flow. NACA Rep. 986, 1950. (Supersedes NACA TN 1944.)
14. Nielsen, Jack N., and Kaattari, George E.: Method for Estimating Lift Interference of Wing-Body Combinations at Supersonic Speeds. NACA RM A51J04, 1951.

TABLE I.- BASIC DATA

M = 2.01					M = 1.61				
α , deg	C_L	C_D	L/D	C_m	α , deg	C_L	C_D	L/D	C_m
Wing 6-0-0									
-2.08	-0.085	0.0255	-3.35	0.0084	-2.08	-0.114	0.0313	-3.65	0.0142
.00	-.002	.0218	-.08	.0002	-.02	-.003	.0270	-.13	.0003
2.10	.081	.0254	3.20	-.0079	2.13	.113	.0310	3.65	-.0143
4.08	.163	.0347	4.69	-.0159	4.20	.226	.0439	5.15	-.0283
5.07	.205	.0417	4.91	-.0202	5.23	.285	.0541	5.26	-.0350
6.07	.244	.0498	4.90	-.0236	6.37	.346	.0674	5.14	-.0421
7.03	.288	.0598	4.82	-.0275	7.25	.394	.0791	4.98	-.0470
Wing 6-33-0									
-2.20	-0.086	0.0228	-3.79	0.0105					
-.02	-.002	.0188	-.11	.0002					
2.13	.079	.0227	3.48	-.0096					
4.18	.160	.0317	5.03	-.0201					
5.23	.199	.0390	5.11	-.0252					
6.22	.240	.0476	5.04	-.0305					
7.27	.281	.0581	4.84	-.0356					
Wing 6-67-0									
-2.08	-0.076	0.0194	-3.91	0.0129					
.02	-.001	.0166	-.03	.0000					
2.15	.075	.0195	3.84	-.0129					
4.13	.148	.0285	5.20	-.0263					
5.13	.185	.0348	5.30	-.0328					
6.15	.222	.0430	5.16	-.0395					
7.15	.259	.0523	4.95	-.0464					
Wing 6-100-0									
-2.05	-0.070	0.0177	-3.95	0.0147	-1.95	-0.086	0.0211	-4.09	0.0218
.03	-.001	.0153	-.08	-.0004	-.02	-.001	.0181	-.07	.0003
2.13	.069	.0182	3.77	-.0158	2.02	.088	.0214	4.11	-.0222
4.10	.136	.0259	5.25	-.0307	4.00	.177	.0322	5.50	-.0445
5.10	.170	.0318	5.36	-.0385	5.17	.228	.0411	5.54	-.0567
6.12	.205	.0393	5.21	-.0462	6.13	.270	.0504	5.36	-.0670
7.12	.240	.0481	4.98	-.0541	3.10	.137	.0264	5.17	-.0345

CONFIDENTIAL

TABLE I.- BASIC DATA - Continued

M = 2.01					M = 1.61				
α , deg	C_L	C_D	L/D	C_m	α , deg	C_L	C_D	L/D	C_m
Wing 6-0-33									
-2.07	-0.080	0.0228	-3.52	0.0098	-2.13	-0.110	0.0279	-3.95	0.0153
.03	-.001	.0195	-.04	.0000	-.02	-.002	.0239	-.09	.0001
2.07	.078	.0231	3.36	-.0095	2.07	.106	.0274	3.87	-.0151
4.02	.155	.0311	4.99	-.0191	4.15	.213	.0389	5.49	-.0297
5.00	.194	.0371	5.22	-.0236	5.32	.274	.0492	5.58	-.0377
5.98	.232	.0446	5.20	-.0280	6.38	.330	.0607	5.43	-.0448
6.95	.272	.0535	5.09	-.0325	7.35	.378	.0722	5.24	-.0509
Wing 6-33-33									
-2.17	-0.081	0.0206	-3.95	0.0116					
.00	-.002	.0170	-.11	.0002					
2.12	.076	.0207	3.65	-.0107					
4.15	.153	.0292	5.23	-.0219					
5.13	.190	.0354	5.36	-.0273					
6.20	.229	.0436	5.24	-.0330					
7.15	.266	.0525	5.07	-.0383					
Wing 6-67-33									
-2.18	-0.078	0.0186	-4.19	0.0139					
.02	-.002	.0151	-.11	.0003					
2.20	.074	.0188	3.92	-.0150					
4.23	.148	.0273	5.42	-.0270					
5.27	.185	.0340	5.44	-.0337					
6.30	.222	.0421	5.28	-.0407					
7.37	.260	.0519	5.01	-.0475					
Wing 6-100-33									
-2.12	-0.070	0.0166	-4.22	0.0147	-2.07	-0.087	0.0196	-4.43	0.0207
.05	-.001	.0140	-.06	-.0001	-.10	-.001	.0167	-.03	.0001
2.15	.068	.0165	4.10	-.0147	2.12	.089	.0200	4.46	-.0213
4.22	.134	.0247	5.44	-.0293	4.18	.180	.0310	5.82	-.0431
5.25	.169	.0308	5.48	-.0368	4.98	.214	.0368	5.81	-.0509
6.17	.203	.0376	5.39	-.0445	6.03	.258	.0460	5.61	-.0613
7.23	.235	.0464	5.07	-.0515	7.15	.304	.0576	5.28	-.0721
					3.07	.132	.0241	5.46	-.0316

~~CONFIDENTIAL~~

TABLE I.- BASIC DATA - Continued

M = 2.01					M = 1.61				
α , deg	C_L	C_D	L/D	C_m	α , deg	C_L	C_D	L/D	C_m
Wing 12-0-0									
0.00	-0.002	0.0262	-0.08	0.0005	-2.27	-0.127	0.0379	-3.34	0.0136
2.03	.078	.0293	2.67	-.0058	-.05	-.004	.0323	-.12	.0005
3.92	.155	.0379	4.10	-.0118	2.18	.115	.0365	3.15	-.0125
6.78	.276	.0615	4.49	-.0214	4.30	.229	.0501	4.57	-.0241
7.78	.321	.0732	4.39	-.0240	5.37	.287	.0605	4.74	-.0296
4.95	.196	.0449	4.37	-.0150	6.47	.347	.0736	4.71	-.0355
-2.03	-.079	.0297	-2.66	.0065	7.53	.406	.0885	4.58	-.0417
Wing 12-33-0									
-2.18	-0.084	0.0255	-3.27	0.0095					
-.02	-.002	.0217	-.09	.0006					
2.13	.079	.0258	3.08	-.0080					
4.25	.160	.0355	4.50	-.0174					
5.25	.199	.0425	4.68	-.0218					
6.25	.239	.0511	4.68	-.0265					
7.32	.280	.0617	4.54	-.0312					
Wing 12-67-0									
-2.13	-0.076	0.0216	-3.51	0.0131					
.03	.000	.0188	-.02	.0008					
2.13	.074	.0217	3.42	-.0116					
4.13	.147	.0305	4.82	-.0243					
5.13	.184	.0370	4.96	-.0306					
6.13	.220	.0450	4.90	-.0370					
7.15	.258	.0543	4.74	-.0435					
Wing 12-100-0									
-2.05	-0.069	0.0195	-3.53	0.0149	-2.17	-0.095	0.0242	-3.92	0.0235
.05	.000	.0168	.00	.0001	.03	-.001	.0204	-.02	.0002
2.13	.069	.0198	3.46	-.0146	2.20	.091	.0241	3.78	-.0226
4.15	.136	.0276	4.91	-.0290	3.23	.140	.0293	4.79	-.0348
5.13	.171	.0337	5.07	-.0369	4.18	.181	.0351	5.16	-.0447
6.13	.205	.0409	5.01	-.0443	5.22	.227	.0434	5.24	-.0555
7.15	.239	.0494	4.83	-.0515	6.20	.268	.0524	5.11	-.0650

TABLE I.- BASIC DATA - Concluded

M = 2.01					M = 1.61				
α , deg	C_L	C_D	L/D	C_m	α , deg	C_L	C_D	L/D	C_m
Wing 12-0-33									
-0.02	0.000	0.0229	0.00	-0.0004	-2.20	-0.114	0.0327	-3.50	0.0130
2.12	.079	.0260	3.02	-.0087	-.03	-.003	.0280	-.10	-.0004
4.10	.156	.0348	4.48	-.0167	2.22	.110	.0319	3.46	-.0140
5.07	.195	.0410	4.74	-.0207	4.27	.217	.0438	4.95	-.0267
6.05	.234	.0488	4.80	-.0248	5.38	.275	.0539	5.10	-.0338
7.08	.276	.0584	4.72	-.0290	6.48	.329	.0653	5.04	-.0404
8.07	.317	.0693	4.57	-.0325	7.50	.380	.0778	4.88	-.0464
-2.05	-.081	.0263	-3.06	.0080					
Wing 12-33-33									
-0.02	-0.001	0.0190	-0.04	-0.0001					
2.13	.077	.0228	3.38	-.0102					
3.17	.116	.0266	4.35	-.0153					
4.18	.153	.0316	4.85	-.0203					
5.20	.192	.0382	5.02	-.0255					
6.20	.229	.0460	4.98	-.0305					
7.22	.270	.0577	4.84	-.0360					
-2.18	-.080	.0227	-3.52	.0101					
Wing 12-67-33									
-0.07	-0.002	0.0167	-0.10	0.0005					
-2.15	-.075	.0200	-3.76	.0131					
2.20	.074	.0203	3.66	-.0164					
4.25	.148	.0292	5.07	-.0254					
5.22	.185	.0355	5.21	-.0320					
6.28	.222	.0437	5.08	-.0386					
7.38	.260	.0535	4.86	-.0453					
Wing 12-100-33									
-2.10	-0.069	0.0178	-3.85	0.0143	-2.52	-0.108	0.0242	-4.46	0.0252
.02	.000	.0151	-.03	.0000	-.05	-.004	.0184	-.20	.0005
2.13	.068	.0177	3.84	-.0144	2.33	.098	.0227	4.31	-.0237
4.17	.135	.0260	5.18	-.0288	4.70	.200	.0365	5.47	-.0468
5.18	.169	.0317	5.32	-.0360	7.36	.300	.0586	5.12	-.0697
6.22	.203	.0391	5.19	-.0433	6.28	.262	.0486	5.38	-.0611
7.25	.237	.0480	4.94	-.0506	3.68	.156	.0295	5.27	-.0369

CONFIDENTIAL

TABLE II.- SUMMARY OF CHARACTERISTICS BASED ON INDIVIDUAL WING AREAS

Wing	M = 2.01						M = 1.61					
	$C_{D_{min}}$	$\frac{C_D - C_{D_{min}}}{C_L^2}$	$C_{L_{\alpha}}$	$\left(\frac{L}{D}\right)_{max}$	$C_{L_{opt}}$	$C_{m_{\alpha}}$	$C_{D_{min}}$	$\frac{C_D - C_{D_{min}}}{C_L^2}$	$C_{L_{\alpha}}$	$\left(\frac{L}{D}\right)_{max}$	$C_{L_{opt}}$	$C_{m_{\alpha}}$
6-0-0	0.0218	0.466	0.0408	4.92	0.220	-0.0039	0.0270	0.334	0.0546	5.26	0.285	-0.0067
6-33-0	.0188	.500	.0382	5.11	.200	-.0050						
6-67-0	.0166	.535	.0360	5.30	.185	-.0062						
6-100-0	.0153	.569	.0332	5.36	.170	-.0075	.0181	.435	.0440	5.55	.210	-.0113
6-0-33	.0195	.469	.0391	5.22	.200	-.0048	.0239	.338	.0516	5.58	.275	-.0071
6-33-33	.0170	.509	.0369	5.36	.187	-.0055						
6-67-33	.0151	.549	.0348	5.44	.170	-.0063						
6-100-33	.0140	.587	.0320	5.48	.150	-.0070	.0166	.444	.0423	5.83	.200	-.0103
12-0-0	.0260	.475	.0392	4.50	.275	-.0031	.0323	.345	.0534	4.74	.310	-.0061
12-33-0	.0217	.505	.0379	4.70	.220	-.0043						
12-67-0	.0188	.534	.0356	4.99	.190	-.0058						
12-100-0	.0168	.562	.0334	5.09	.175	-.0071	.0204	.444	.0431	5.25	.225	-.0109
12-0-33	.0229	.475	.0389	4.81	.240	-.0040	.0280	.345	.0509	5.10	.300	-.0065
12-33-33	.0190	.511	.0370	5.03	.210	-.0049						
12-67-33	.0167	.545	.0348	5.21	.185	-.0060						
12-100-33	.0151	.580	.0324	5.33	.170	-.0069	.0184	.448	.0422	5.49	.215	-.0101

TABLE III.- SUMMARY OF CHARACTERISTICS BASED ON AREA OF THE X-0-0 WING

Wing	M = 2.01						M = 1.61					
	$C_{D_{min}}$	$\frac{C_D - C_{D_{min}}}{C_L^2}$	$C_{L_{\alpha}}$	$\left(\frac{L}{D}\right)_{max}$	$C_{L_{opt}}$	c.p. at $\alpha = 2^\circ$ (a)	$C_{D_{min}}$	$\frac{C_D - C_{D_{min}}}{C_L^2}$	$C_{L_{\alpha}}$	$\left(\frac{L}{D}\right)_{max}$	$C_{L_{opt}}$	c.p. at $\alpha = 2^\circ$ (a)
6-0-0	0.0218	0.466	0.0408	4.92	0.220	0.345	0.0270	0.334	0.0546	5.26	0.285	0.374
6-33-0	.0210	.450	.0425	5.11	.200	.296						
6-67-0	.0203	.438	.0440	5.30	.185	.250						
6-100-0	.0204	.427	.0443	5.36	.170	.211	.0241	.326	.0587	5.55	.210	.254
6-0-33	.0217	.421	.0435	5.22	.200	.400	.0266	.304	.0575	5.58	.275	.423
6-33-33	.0208	.416	.0451	5.36	.187	.346						
6-67-33	.0201	.412	.0464	5.44	.170	.301						
6-100-33	.0202	.406	.0462	5.48	.150	.254	.0240	.307	.0611	5.83	.200	.295
12-0-0	.0260	.475	.0392	4.50	.275	.323	.0323	.345	.0534	4.74	.310	.356
12-33-0	.0242	.454	.0421	4.70	.220	.270						
12-67-0	.0230	.437	.0435	4.99	.190	.225						
12-100-0	.0224	.421	.0445	5.09	.175	.186	.0272	.333	.0575	5.25	.225	.245
12-0-33	.0255	.427	.0432	4.81	.240	.382	.0311	.310	.0566	5.10	.300	.403
12-33-33	.0232	.418	.0452	5.03	.210	.334						
12-67-33	.0223	.409	.0464	5.21	.185	.290						
12-100-33	.0218	.401	.0468	5.33	.170	.245	.0266	.310	.0610	5.49	.215	.300

^aFraction of \bar{c} of the X-0-0 wing.

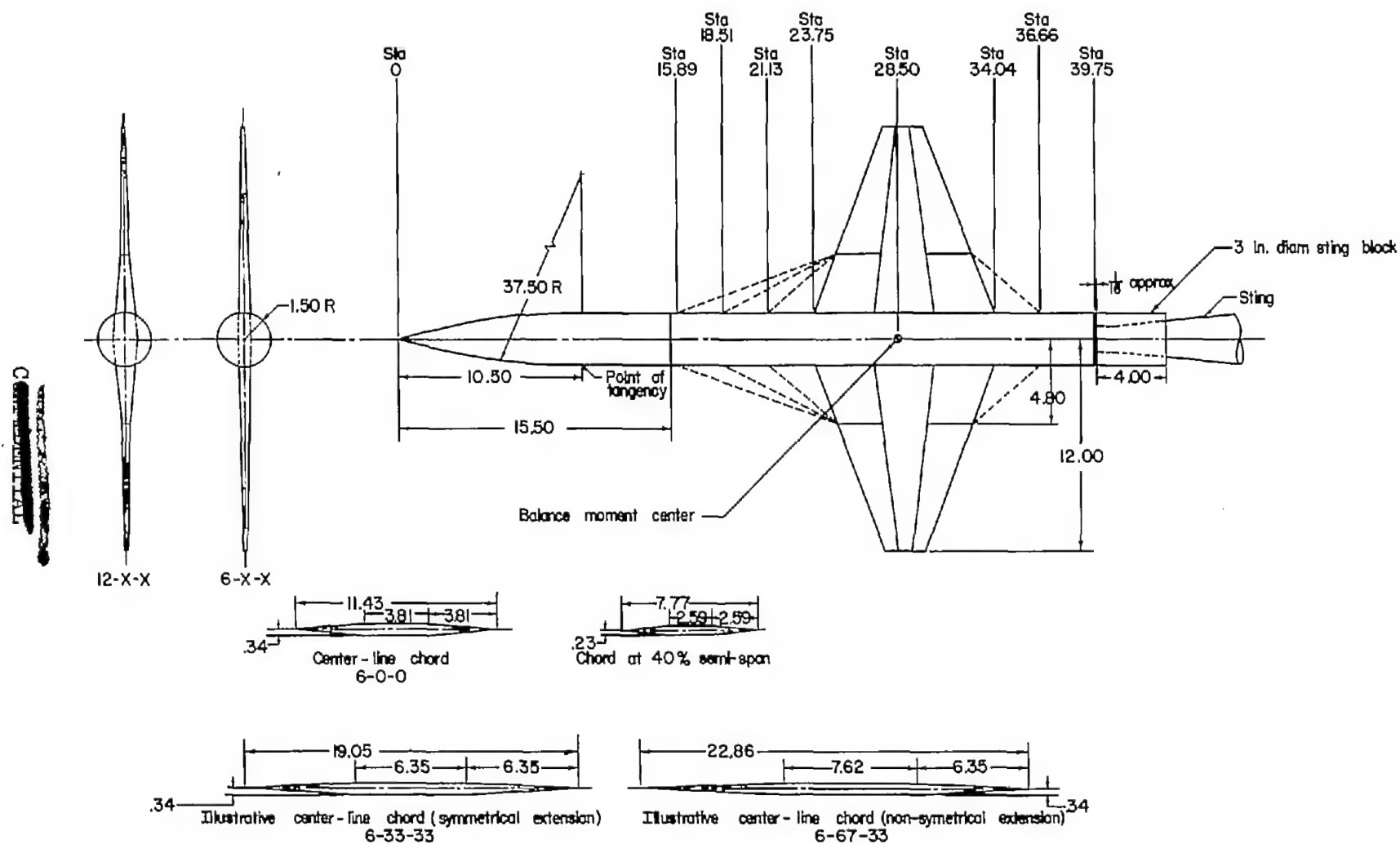


Figure 1.- Schematic layout of model. (All dimensions in inches, unless otherwise specified.)

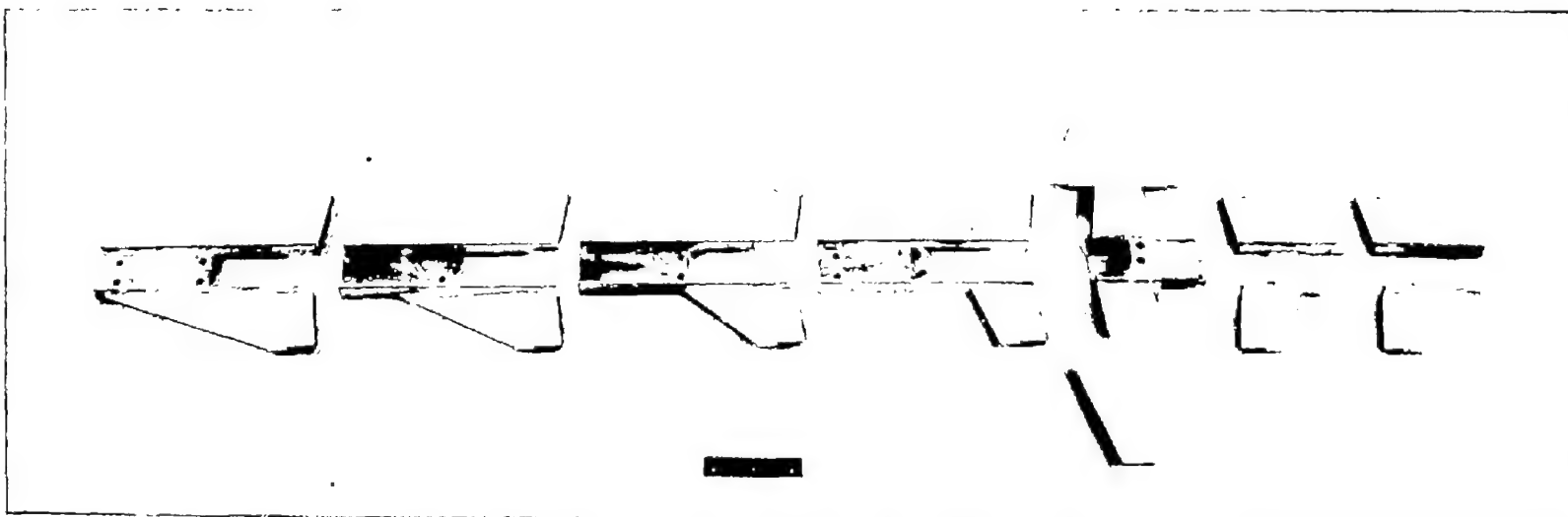


Figure 2.- Details of wing assembly.

L-80694

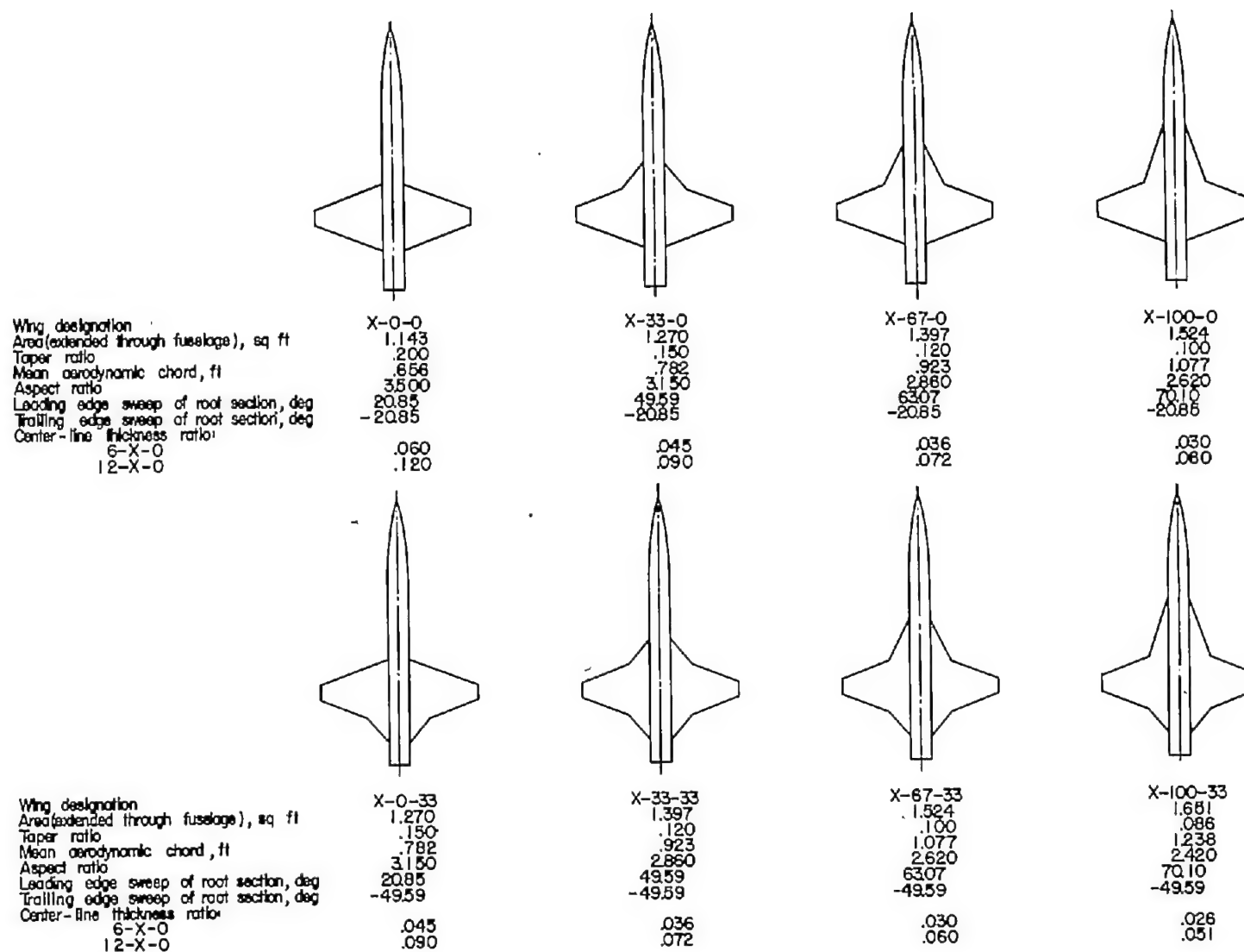
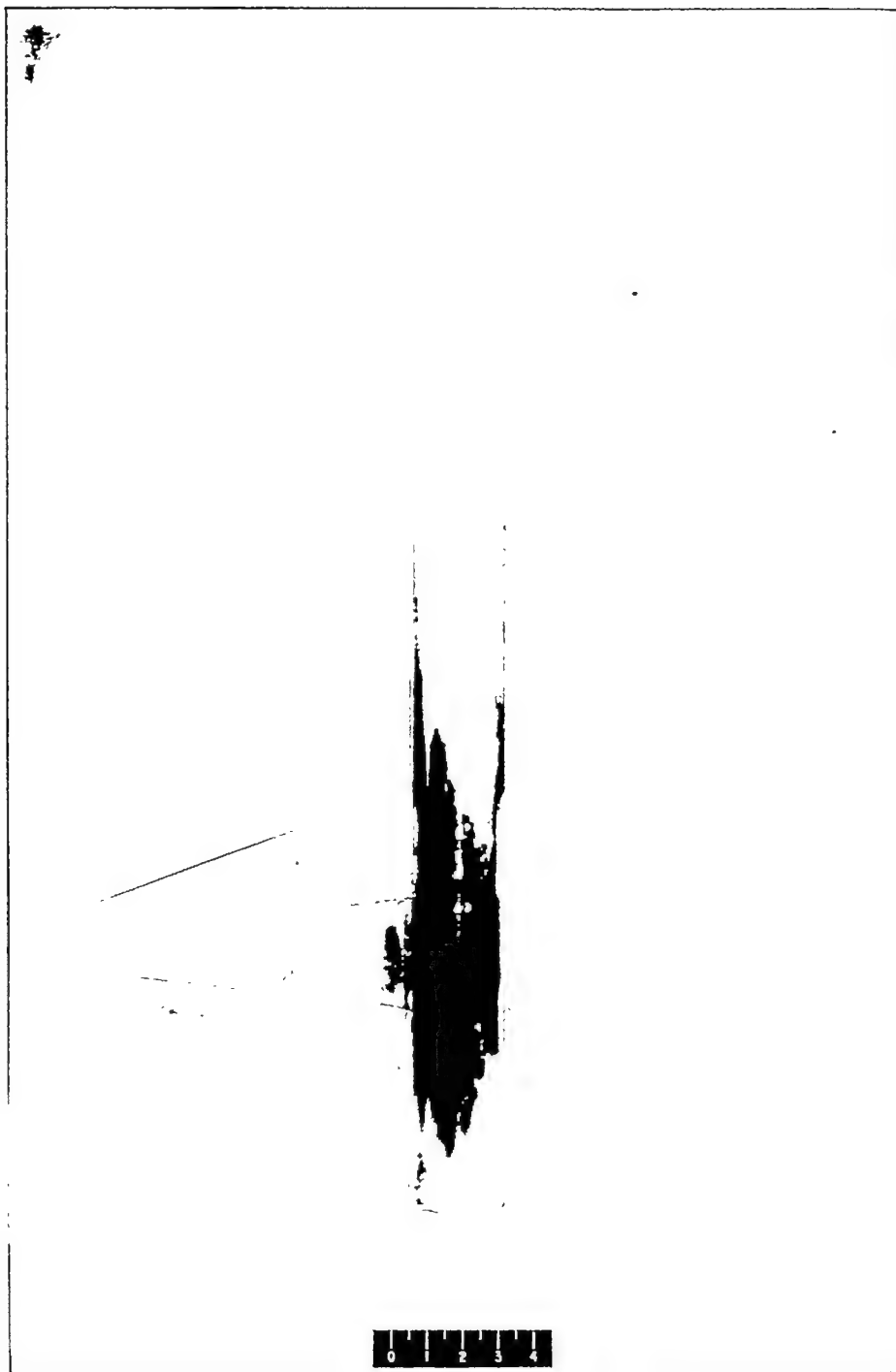


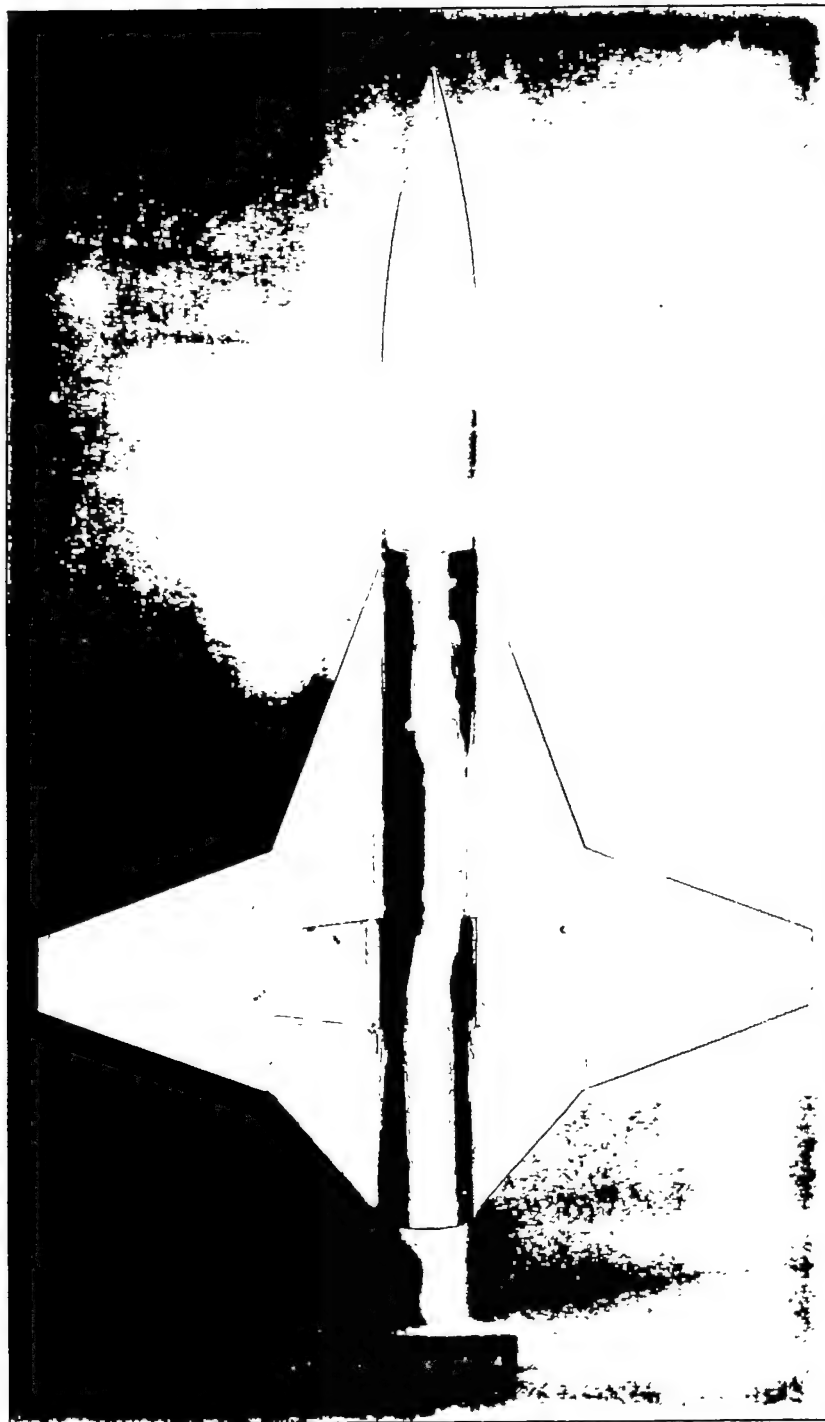
Figure 3.- Geometry of wing-body combinations.



(a) The 6-0-0 wing in combination with body.

L-80693

Figure 4.- Wing-body configurations.



L-80692

(b) The 6-100-33 wing in combination with body.

Figure 4.- Concluded.

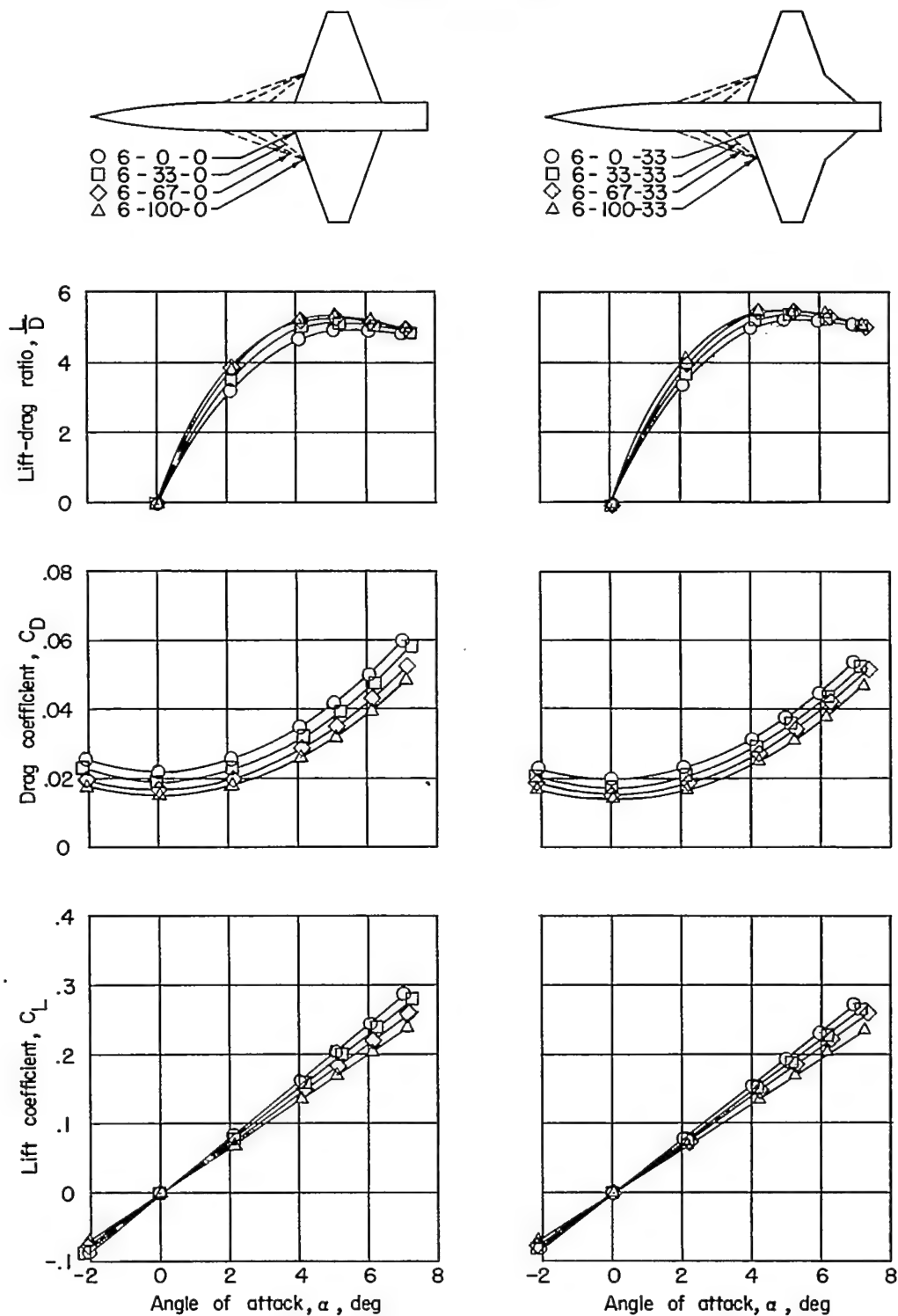
(a) $M = 2.01$.

Figure 5.- Lift and drag characteristics for 6-X-X wing-body configurations.

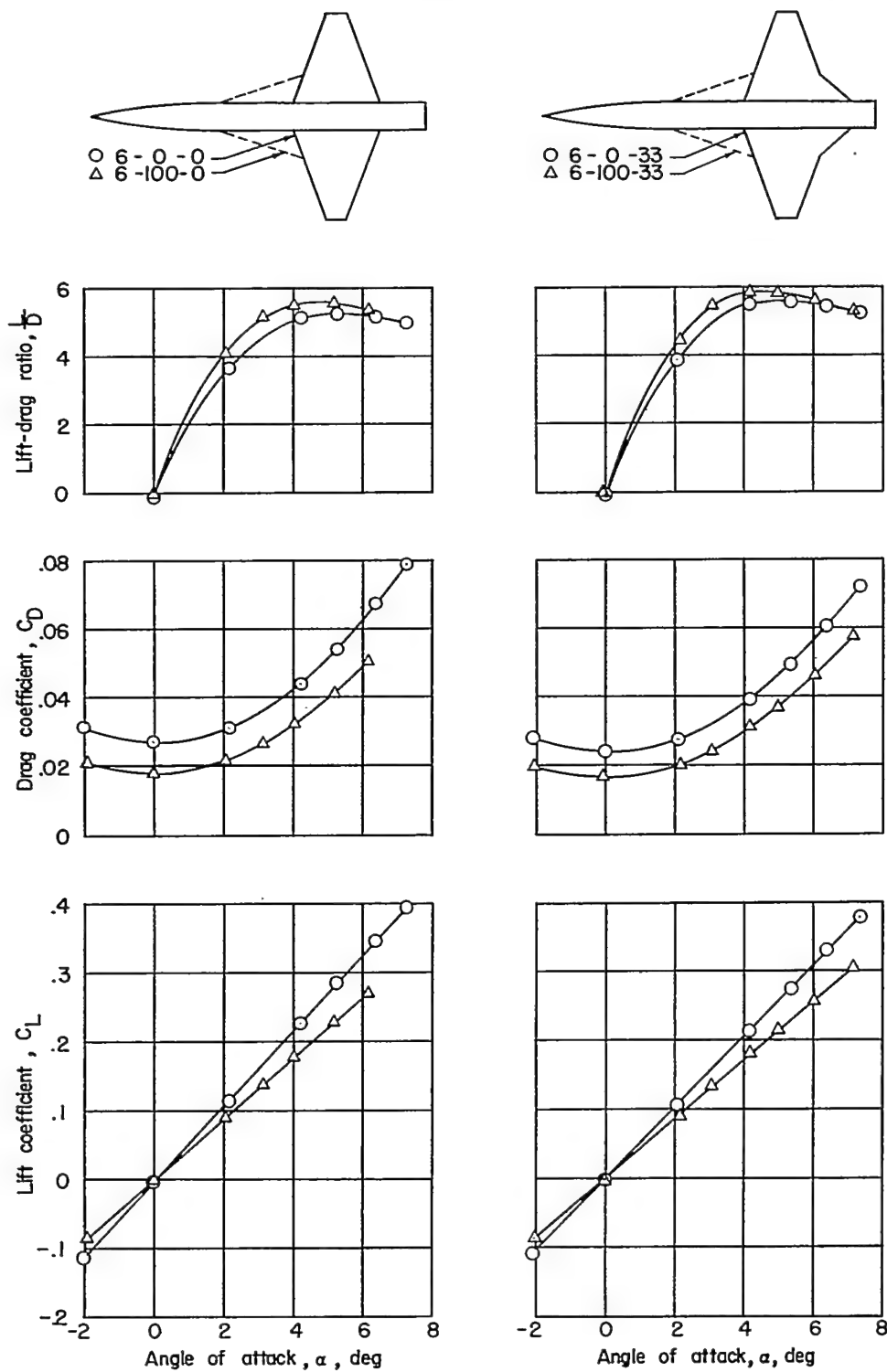
~~CONFIDENTIAL~~(b) $M = 1.61$.

Figure 5.- Concluded.

~~CONFIDENTIAL~~

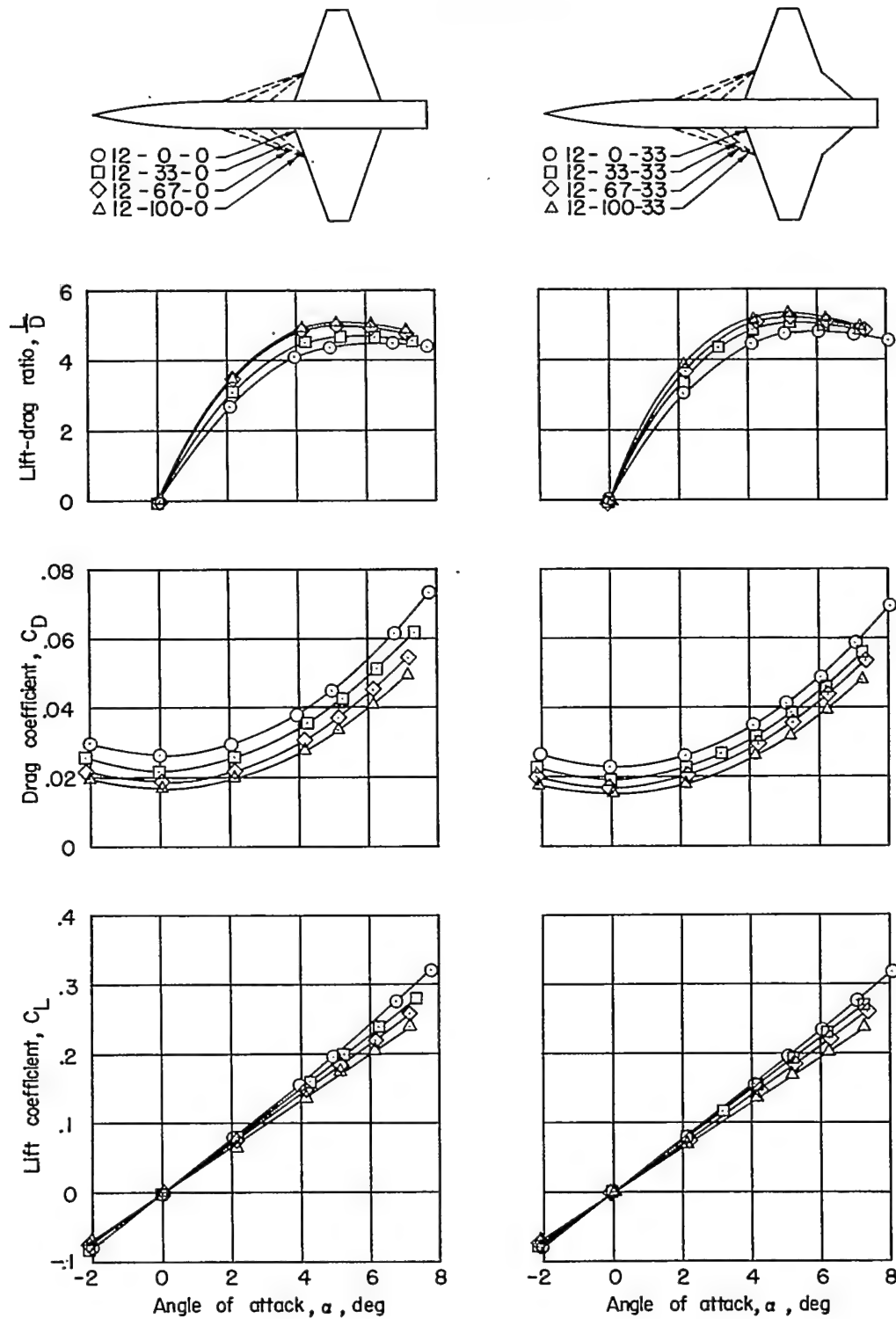
(a) $M = 2.01$.

Figure 6.- Lift and drag characteristics for 12-X-X wing-body configurations.

~~CONFIDENTIAL~~

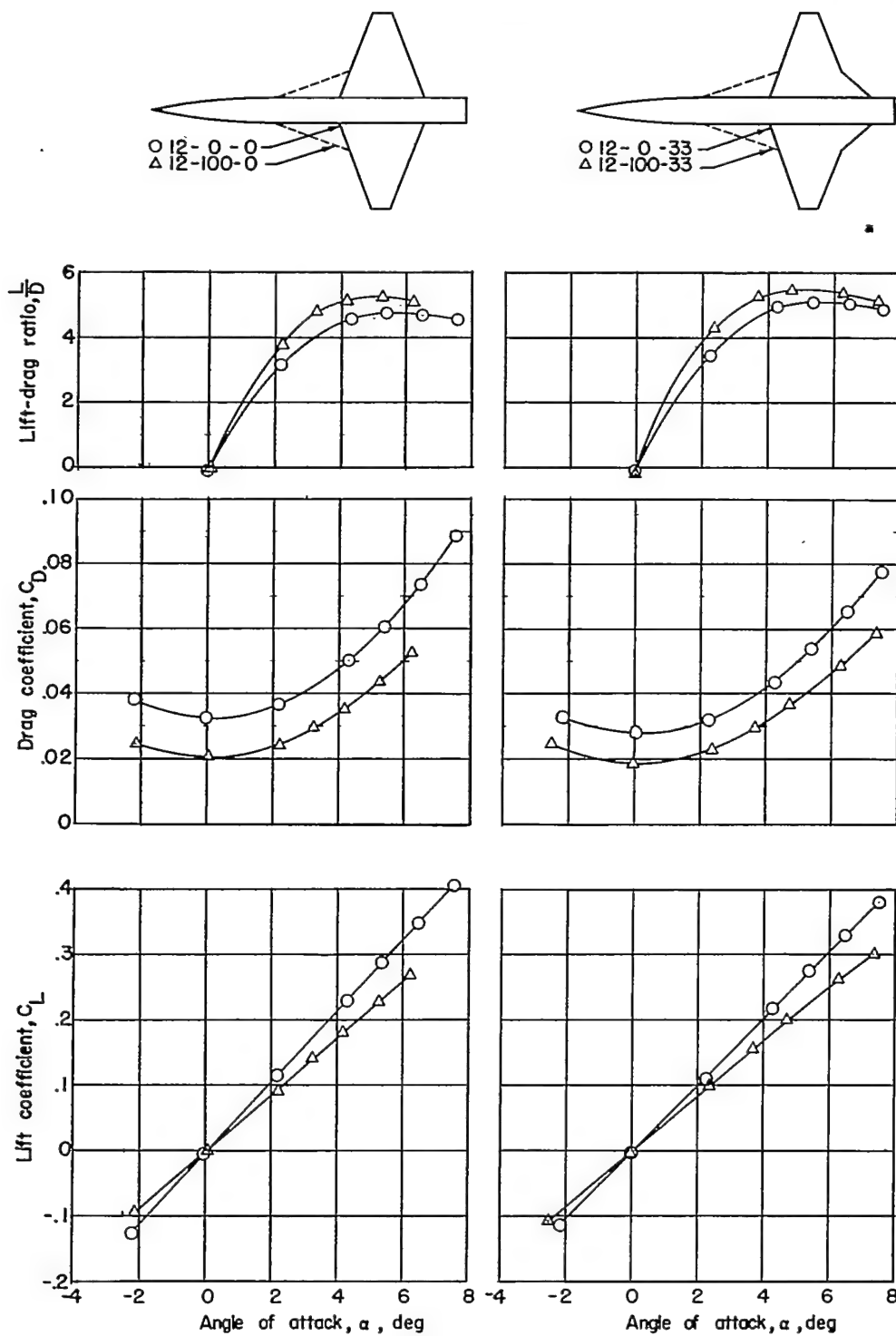
(b) $M = 1.61$.

Figure 6.- Concluded.

~~CONFIDENTIAL~~

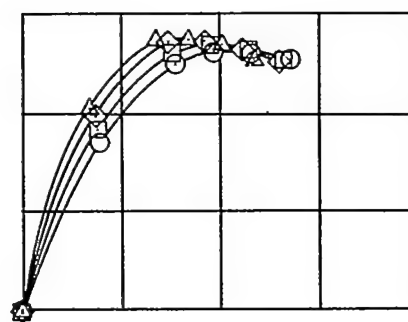
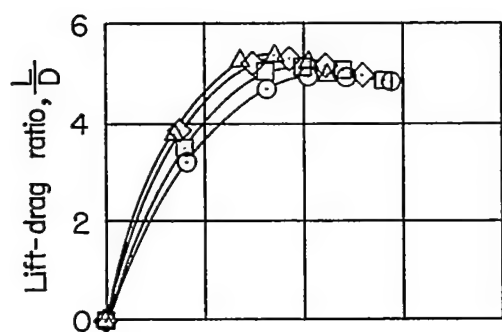
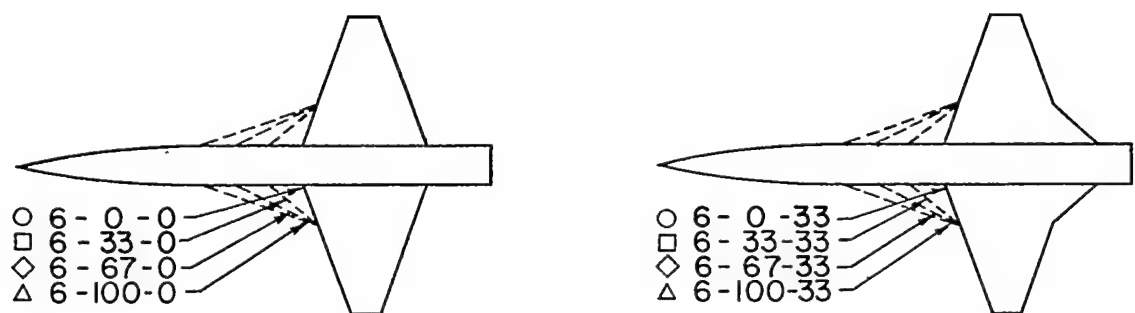
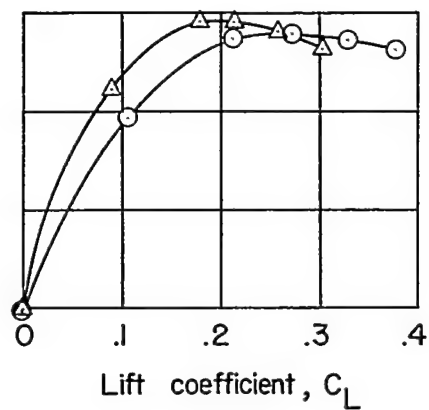
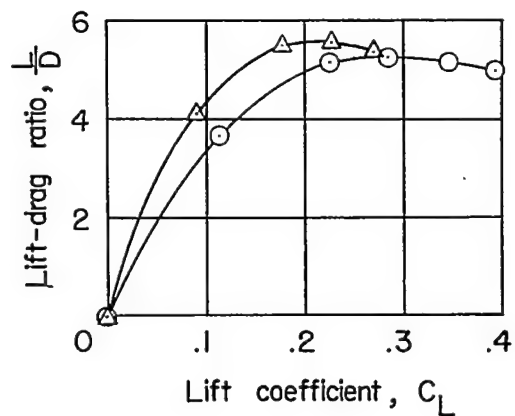
(a) $M = 2.01$.(b) $M = 1.61$.

Figure 7.- Lift-drag ratios for 6-X-X wing-body configurations.

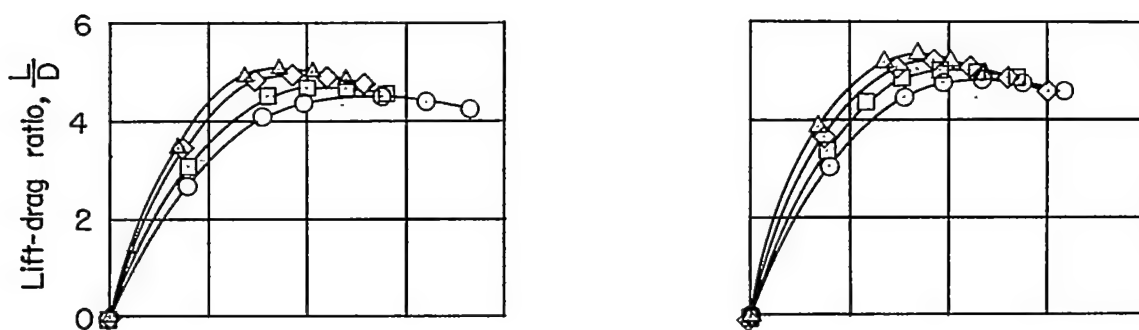
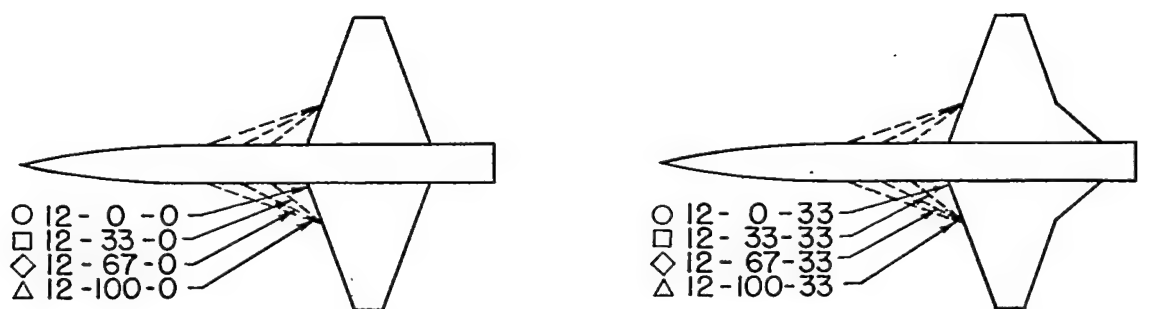
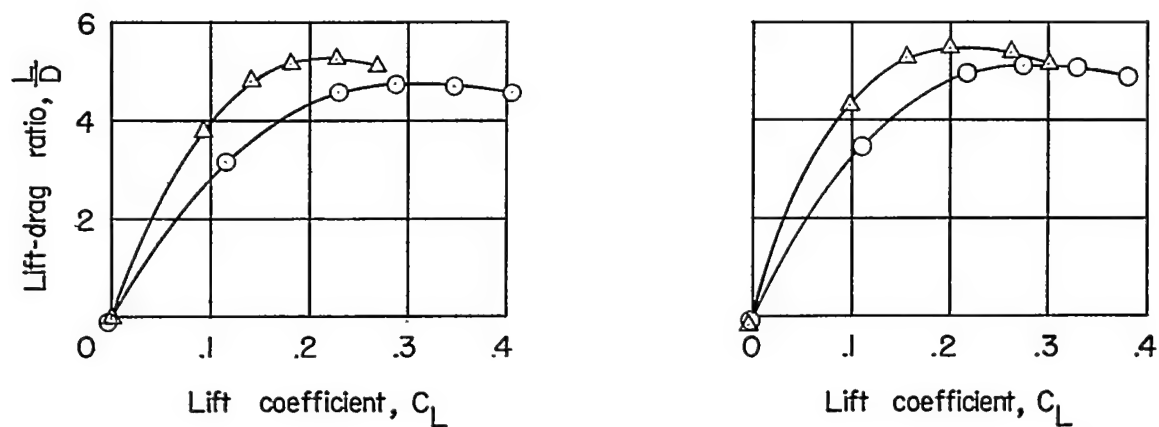
(a) $M = 2.01$.(b) $M = 1.61$.

Figure 8.- Lift-drag ratios for 12-X-X wing-body configurations.

CONFIDENTIAL

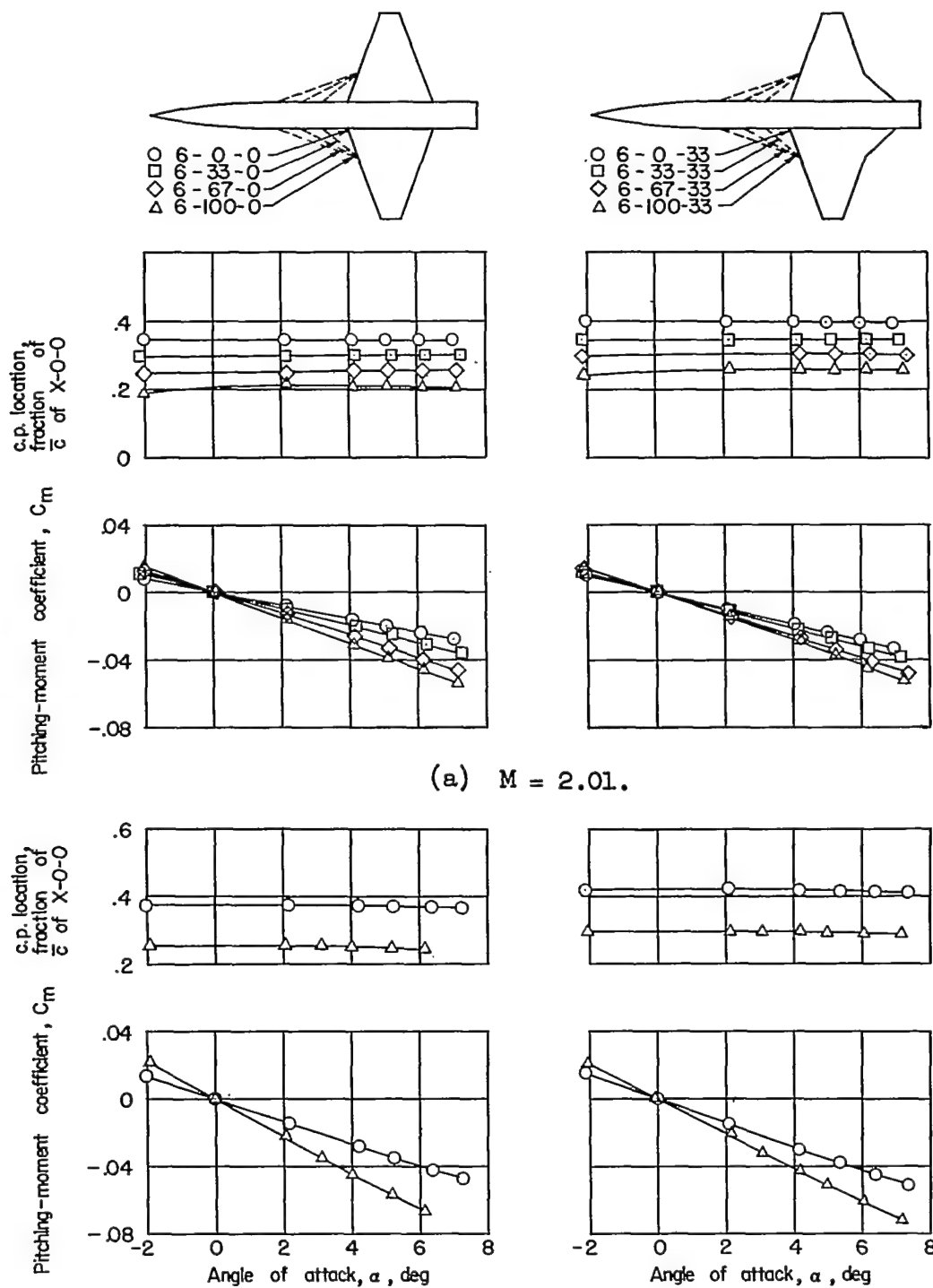


Figure 9.- Pitching-moment and center-of-pressure characteristics of 6-X-X wing-body configurations.

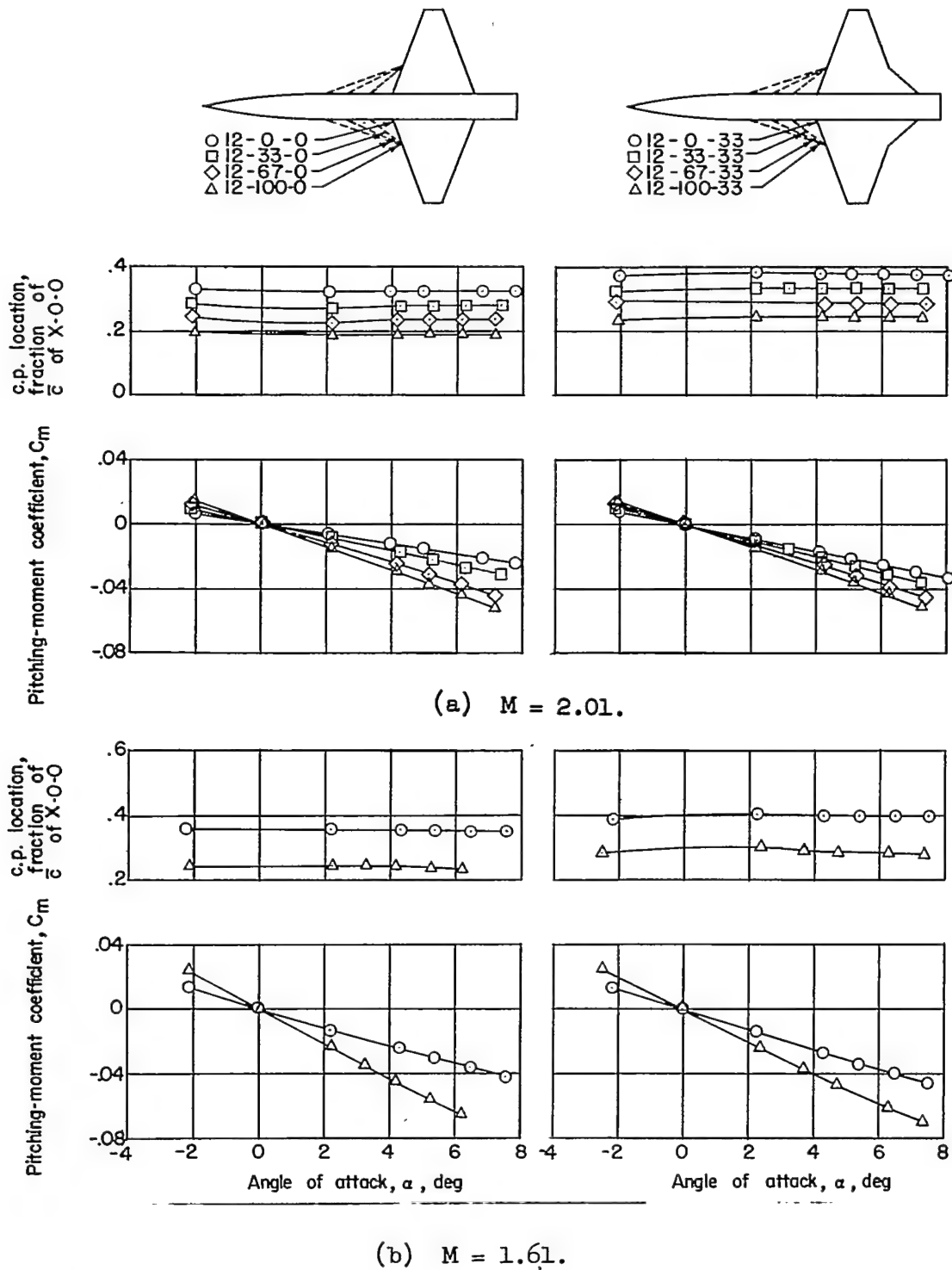
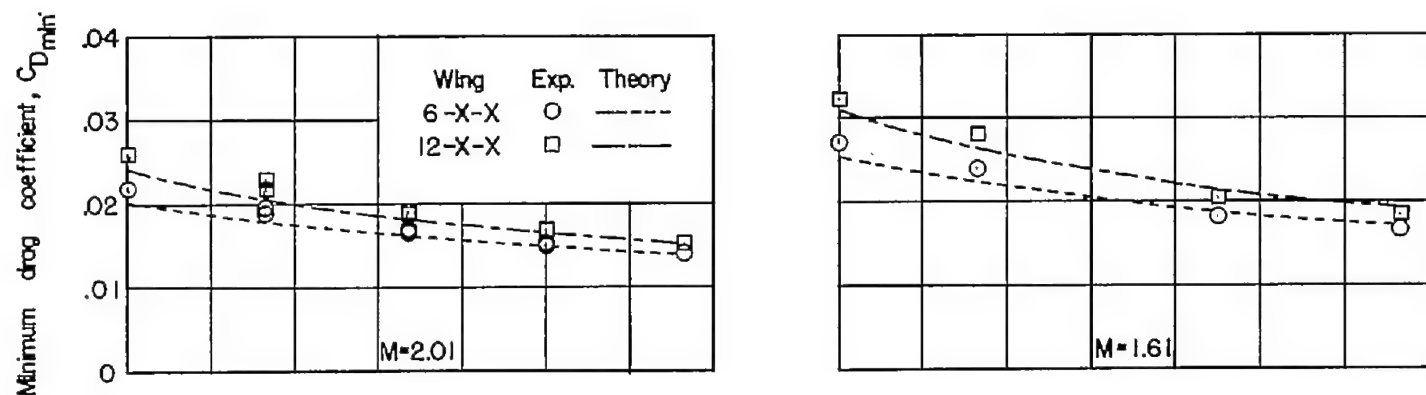
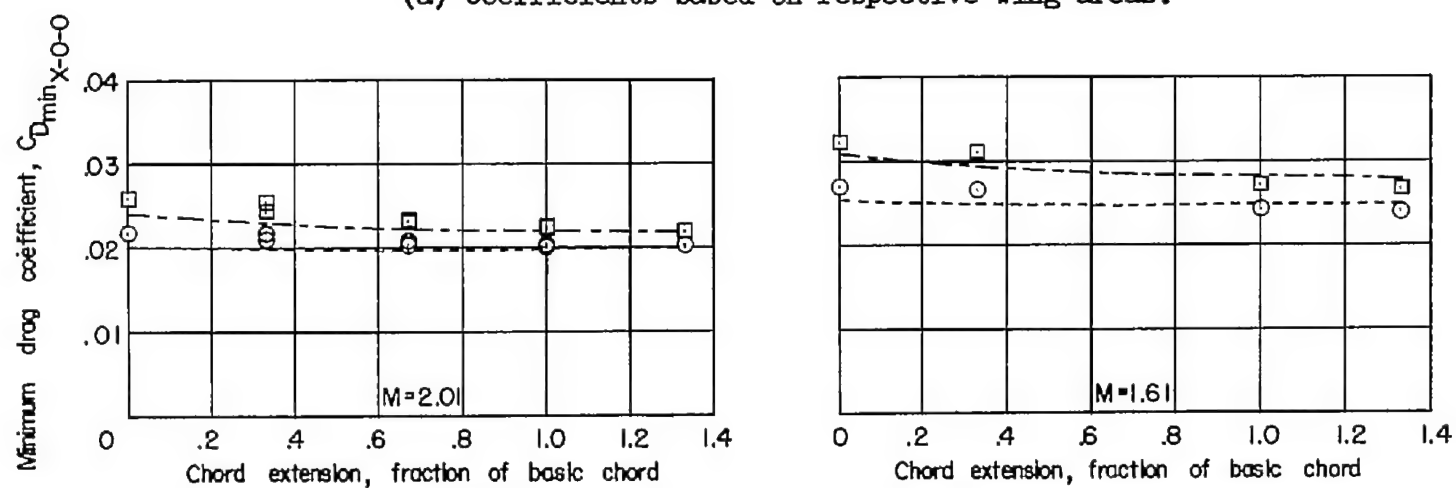


Figure 10.- Pitching-moment and center-of-pressure characteristics for 12-X-X wing-body configurations.

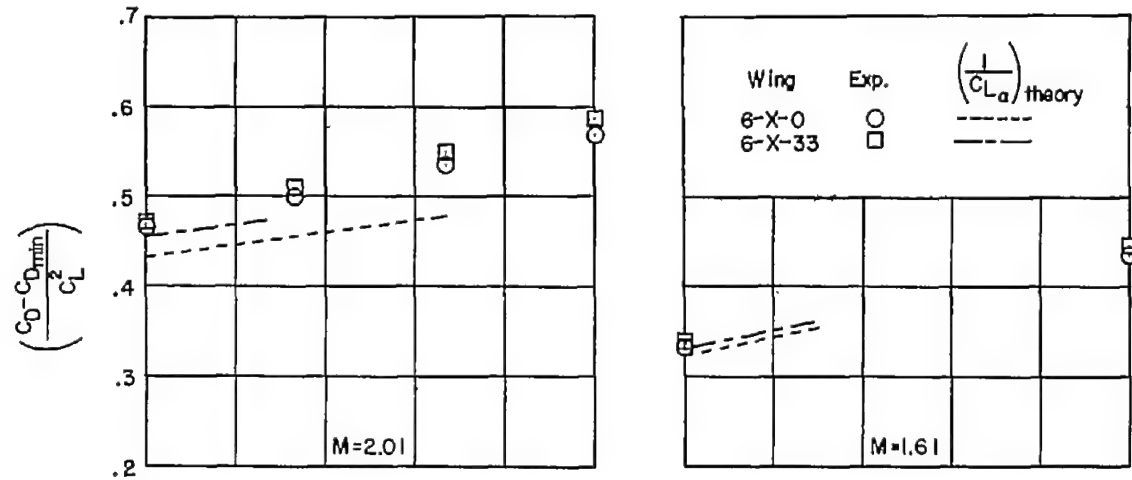


(a) Coefficients based on respective wing areas.

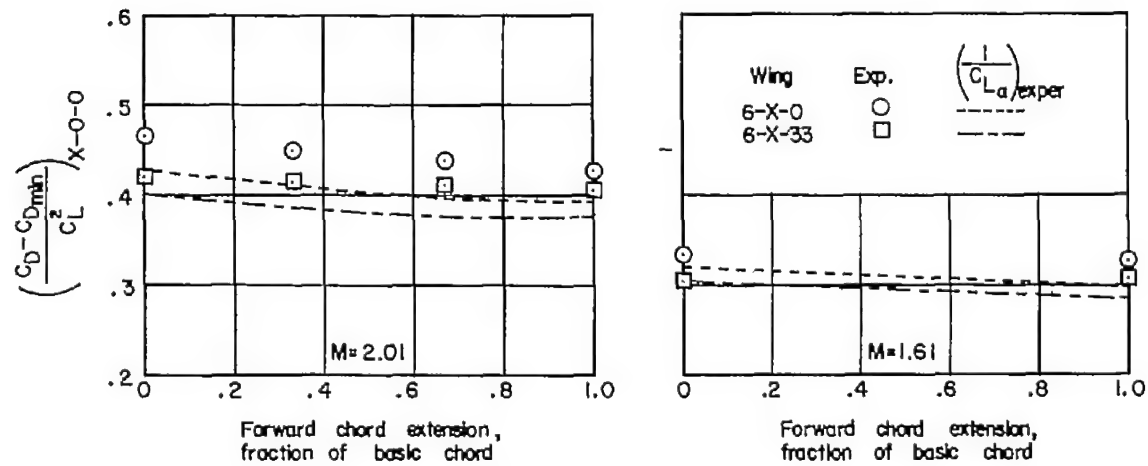


(b) Coefficients based on area of X-0-0 wing.

Figure 11.- Minimum drag characteristics of 6-X-X and 12-X-X wing-body configurations.

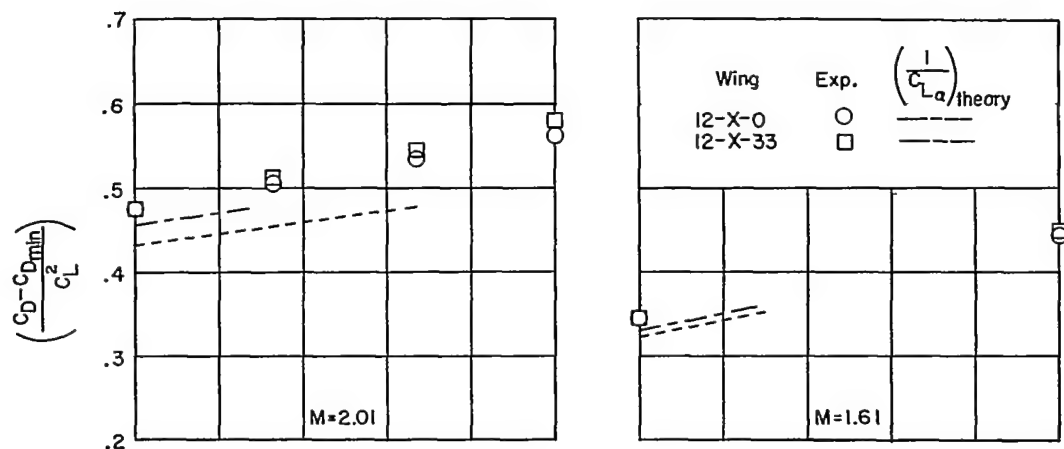


(a) Parameter based on respective wing areas.

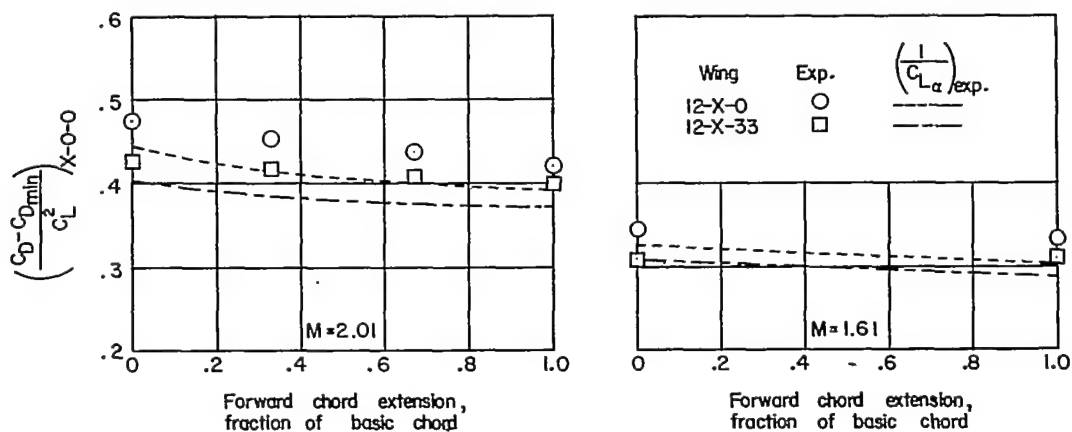


(b) Parameter based on area of X-0-0 wing.

Figure 12.- Drag-due-to-lift characteristics of 6-X-X wing-body configurations.

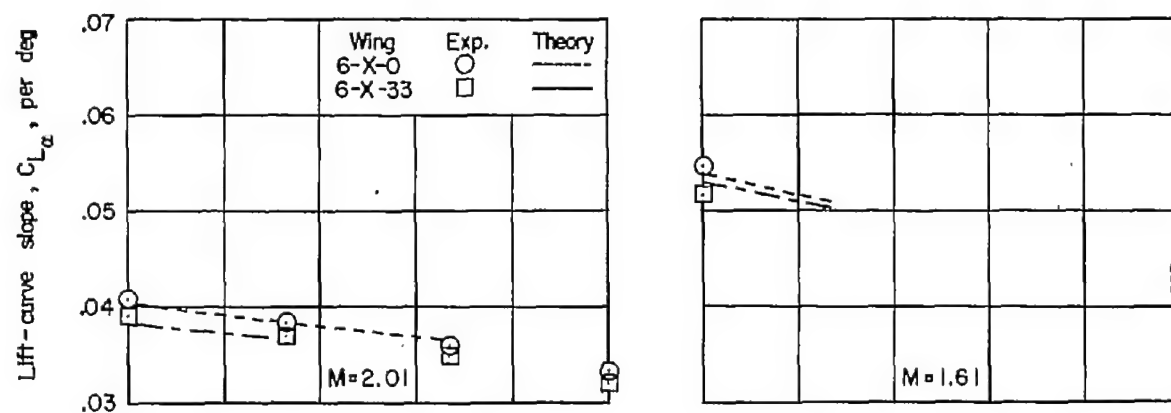


(a) Parameter based on respective wing areas.

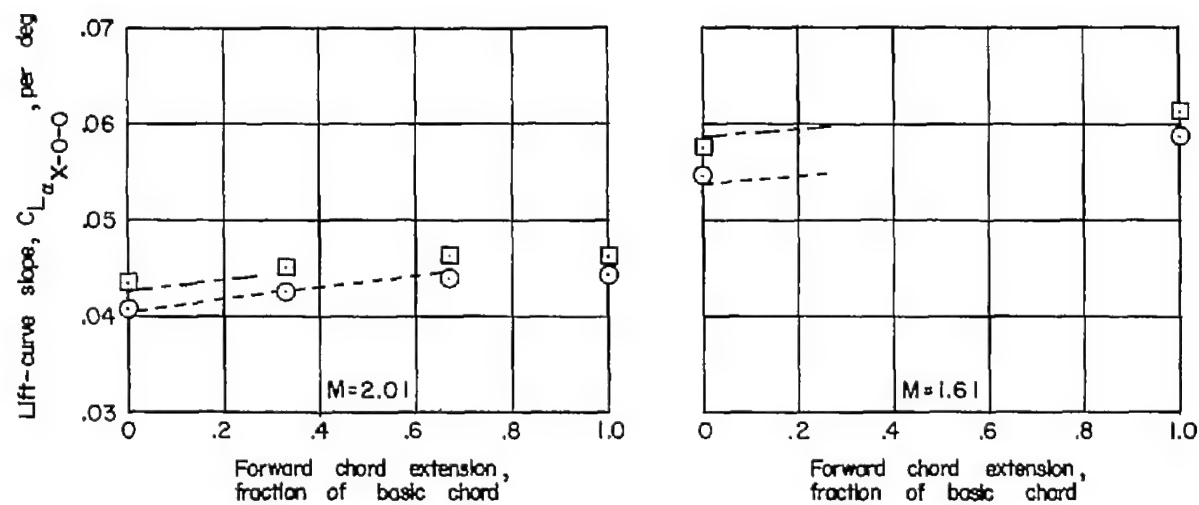


(b) Parameter based on area of X-0-0 wing.

Figure 13.- Drag-due-to-lift characteristics of 12-X-X wing-body configurations.

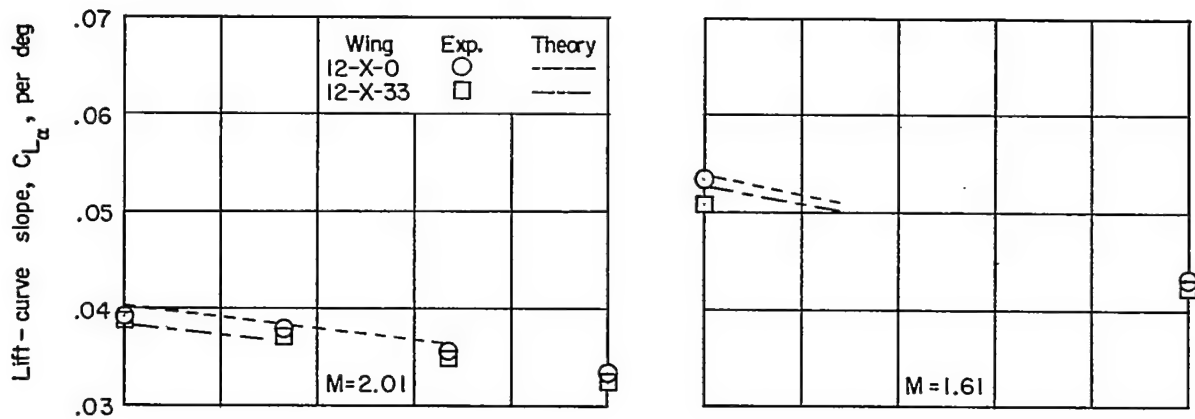


(a) Coefficients based on respective wing areas.

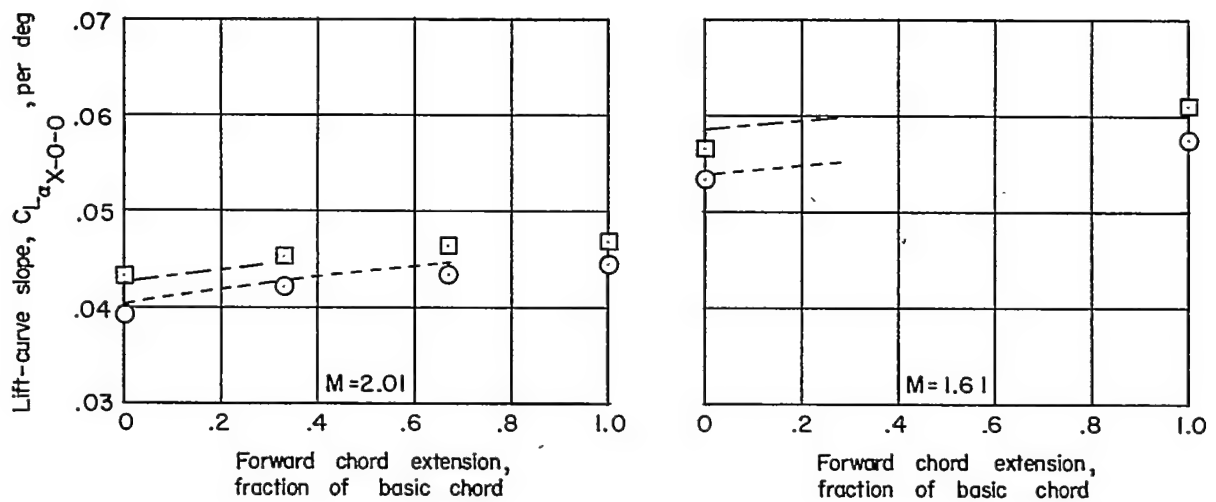


(b) Coefficients based on area of X-0-0 wing.

Figure 14.- Lift-curve slopes of 6-X-X wing-body configurations.



(a) Coefficients based on respective wing areas.



(b) Coefficients based on area of X-0-0 wing.

Figure 15.- Lift-curve slopes of 12-X-X wing-body configurations.

CONFIDENTIAL

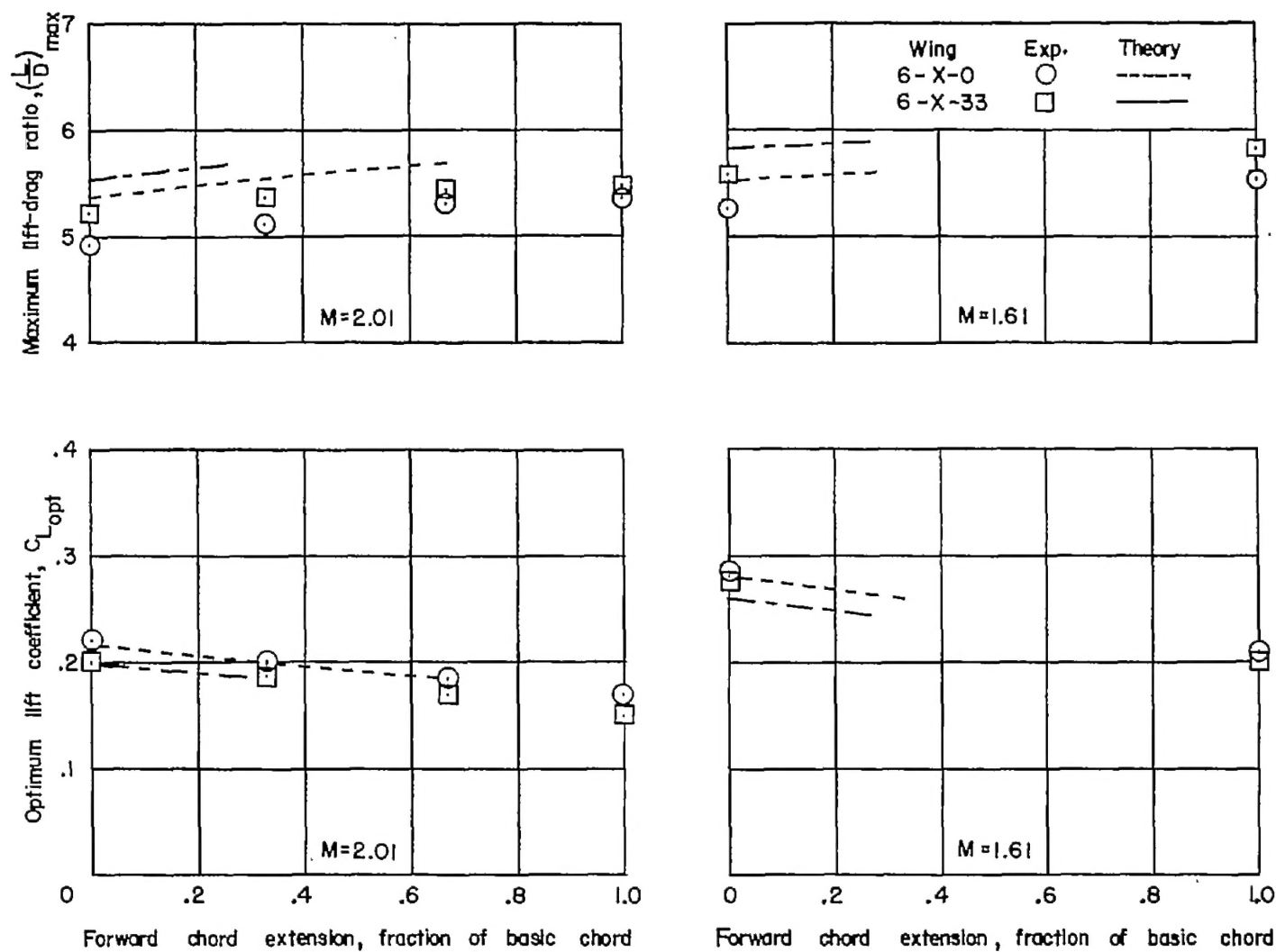


Figure 16.- Maximum lift-drag ratios and optimum lift coefficients for 6-X-X wing-body configurations.

CONFIDENTIAL

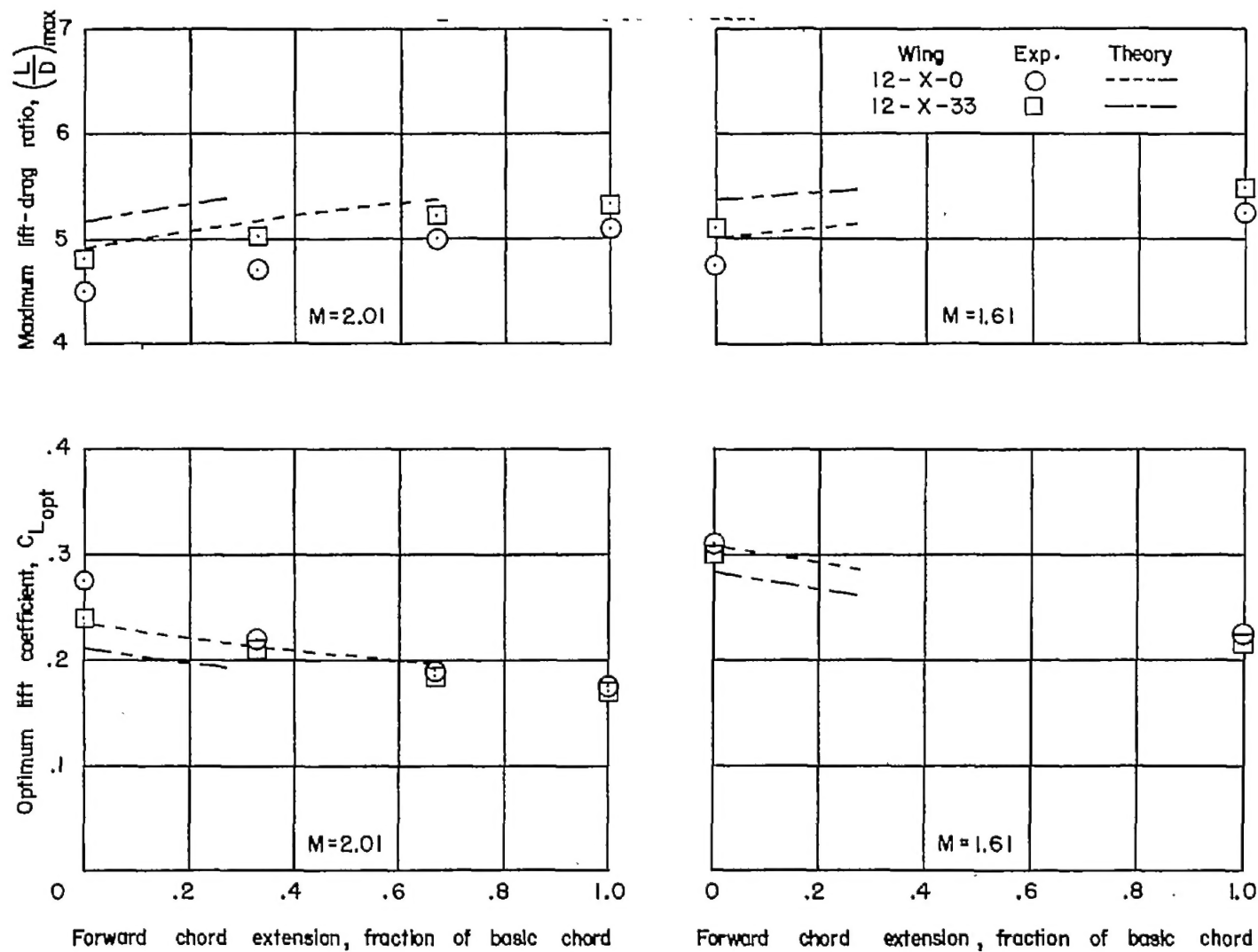


Figure 17.- Maximum lift-drag ratios and optimum lift coefficients for 12-X-X wing-body configurations.

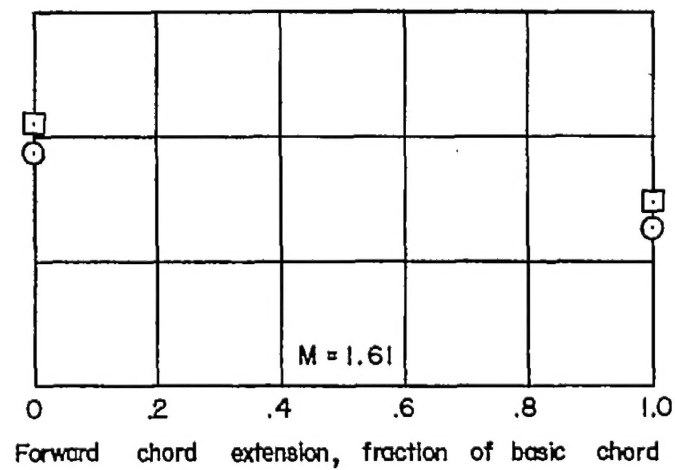
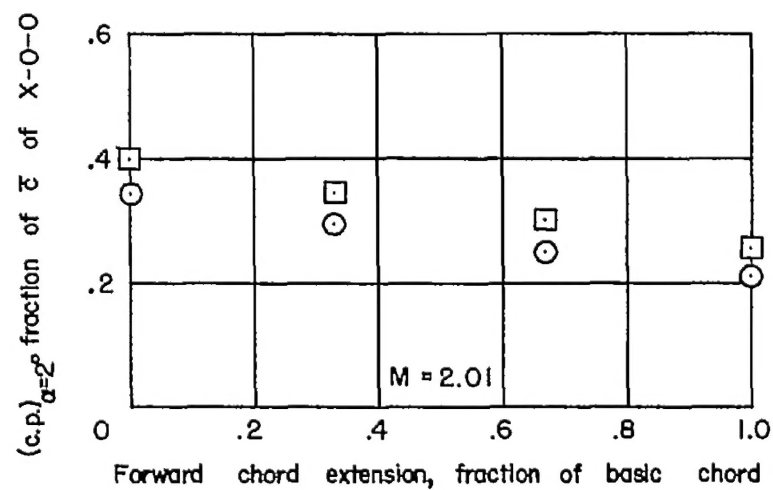
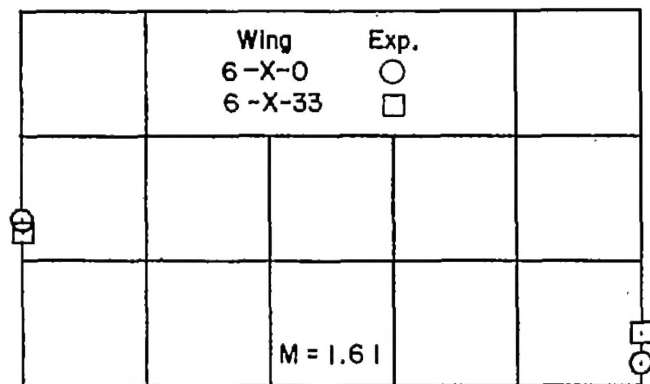
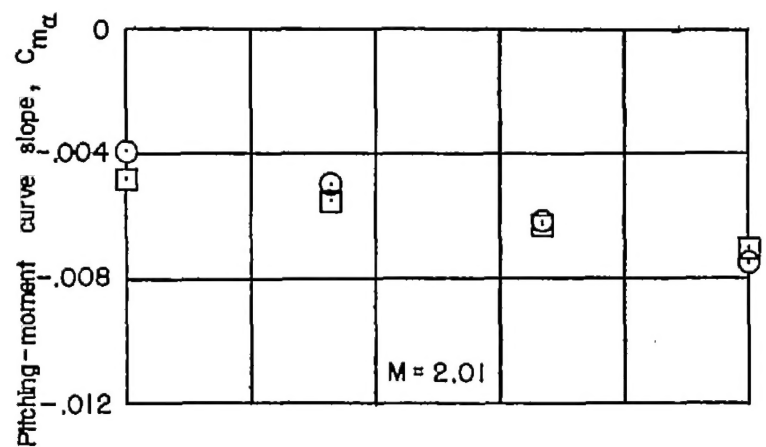


Figure 18.- Pitching-moment-curve slope and representative center-of-pressure characteristics for 6-X-X wing-body configurations.

CONFIDENTIAL

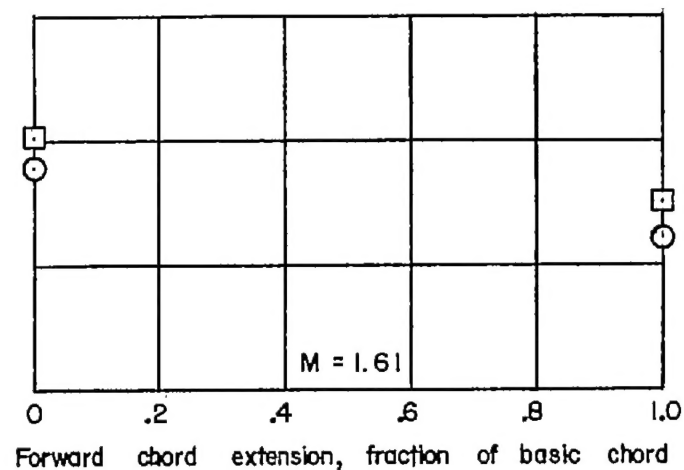
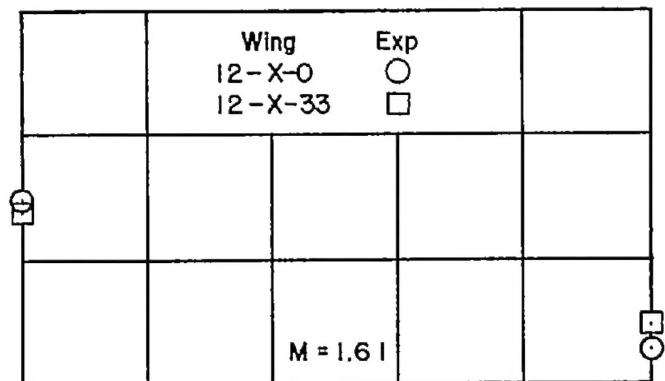
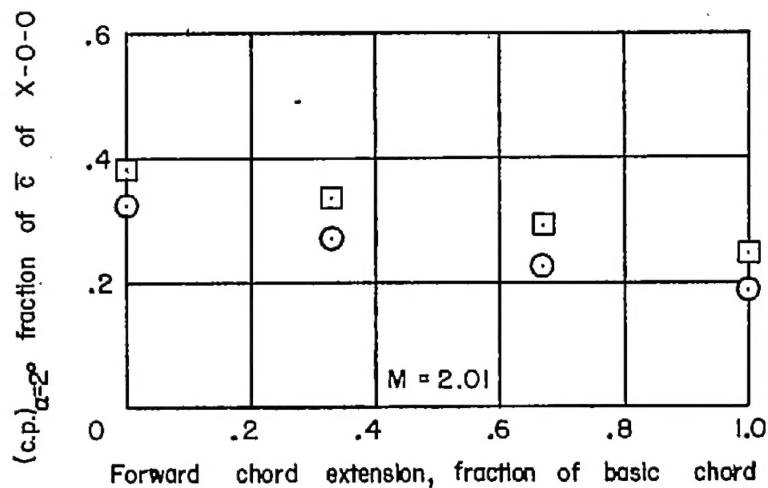
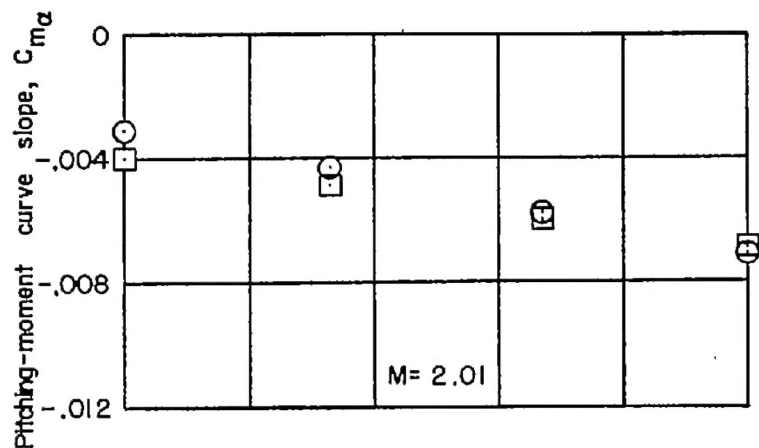


Figure 19.- Pitching-moment-curve slope and representative center-of-pressure characteristics for 12-X-X wing-body configurations.

CONFIDENTIAL